

A Topological Approach to Assembling Strands-Based DNA Tetrahedra

Shuya Liu, Luxuan Guo, Hui Bai, Jincheng Hao*

*School of Chemistry and Chemical Engineering,
Shandong University, Jinan 250018, P. R. China*

liushuya@sdu.edu.cn, jhao@sdu.edu.cn

(Received April 27, 2018)

Abstract

With the rapid development of DNA nanotechnology, DNA polyhedra have been reported and widely applied in chemical biology, analytical chemistry, medicine and materials science. Our goal in this paper is to determine all permissible topological structures for DNA tetrahedra with double-helical edges, which have been partially realized by multiple appropriately designed oligonucleotides. Here four types of oriented twist tangles with even or odd number are designed as basic building blocks to assemble tetrahedral links as the mathematical models for DNA tetrahedra. As a result, there are a total of 26 different link types to be identified from all generated tetrahedral links. Each type includes infinite many tetrahedral links by changing the number of building blocks on each edge. Furthermore, the chirality of these links is discussed and all determined by calculating some invariants such as crossing number, twist number and HOMFLY polynomial. In particular, four achiral tetrahedral links are firstly given by employing the association of tetrahedral link diagrams and their dual link diagrams. Our work provides a list of candidates for further synthesized DNA tetrahedra with required topological structures.

1 Introduction

Molecular recognition capability, rigidity and flexibility of DNA make it an attractive, versatile and highly programmable building block for constructing 3D nanoscale materials [1–3]. Over the past decades, DNA molecules with polyhedral shapes have been successfully synthesized and commonly studied such as tetrahedra [4–9], cubes [10, 11],

*Corresponding author.

octahedra [12–14], dodecahedra [15], icosahedra [16, 17], truncated octahedra [18] and so on. Tetrahedra, as the simplest Platonic polyhedra, were realized mainly using three methods including individual strands-based assembly, tiled-based hierarchical assembly and scaffolded DNA origami [19]. In these works, DNA tetrahedra with a double helix on each edge [5, 6], assembled by multiple synthetic DNA single strands with designed sequences, become a popular candidate for various applications such as nuclear magnetic resonance imaging, molecular diagnosis and targeting drug delivery because they are easily synthesized and also have very high yield, fairly good stereoselectivity as well as outstanding stability [19–21]. Moreover, these tetrahedral molecules can be easily targeted decoration in multiple sites and also be used as the building blocks for more complicated nanostructures [4, 19]. We note that such molecules all have nontrivial topological structures embedded in three dimension space \mathbb{R}^3 , which has a close influence on structural stability, the number of oligonucleotides used in the experiment, dependency on stoichiometry and so on. Hence it becomes necessary to answer which topological structures these DNA molecules will possibly allow. This question is addressed in the present study.

Knot theory [22], the study of simple closed curves in \mathbb{R}^3 , has been proven to be successful in describing knotted and linked molecules [23, 24]. Polyhedral links [25], introduced as the mathematical models for DNA polyhedra, are the interlocked and interlinked architectures formed by simply treating DNA as a strand. To date, a variety of polyhedral links [26–43] have been constructed to describe the topological structures of polyhedral molecules with complete helical-turn edges. However, there is very little research addressed to model DNA polyhedra with incomplete helical-turn edges due to the uncertain orientations of the constructed mathematical links [44]. Hence it is almost impossible to give all possible existing polyhedral links based on any given polyhedron. In this paper, four oriented twist tangles, each designed as two antiparallel oriented strands with even or odd twist number, are used as basic building blocks to assemble all permissible topological structures for DNA tetrahedra with double-helical frames. As a result, there are 26 different link types for oriented link diagrams constructed from tetrahedral graph.

Link invariants, as important tools in knot theory to determine whether two links are equivalent, play the significant roles in classifying and predicting molecular catenanes and knots [39, 45, 46]. In this paper, the component number and crossing number as two

link invariants, and the twist number as a regular isotopy invariant of oriented link diagrams are all given, which provide a sketchable description and classification for oriented tetrahedral links. Furthermore, there is an inequality in terms of the crossing number and twist number for alternating link diagrams, giving a necessary condition for chiral links [47]. Using this inequality, the chirality of most tetrahedral links can be easily determined. However, there are six types of chiral tetrahedral links, we have to resort to a more powerful invariant, the HOMFLY polynomial [48–50]. Here the lowest-degree terms of z for HOMFLY polynomials are calculated and shown to be asymmetrical in order to prove the chirality of these links. For achiral links, there is still no an effective approach to identifying them. In this paper, we employ the association between tetrahedral link diagrams and their dual link diagrams by using the well-known Reidemeister moves [22], and show that there are four types of tetrahedral links to be achiral. It is worth noting that these achiral links are constructed firstly, which affords an expectation for synthesizing achiral catenanes. Hence our works provide a theoretical framework for assembling DNA tetrahedra with required topological structures, and also give new insight into the topological structures for DNA Tetrahedra with double-helical frames.

2 Construction method of tetrahedral links

In this section, a mathematical method is proposed to determine all topological structures of tetrahedral links. We will begin with some notations and basic definitions [22, 51].

2.1 Graphs and link diagrams

In graph theory, a *planar graph* G is a graph that can be drawn in the plane with no edge crossings. Such a drawing is called a *plane graph* of G . Since all convex polyhedra are 3-connected planar graphs [52], each of them has an embedding on the plane. Such an embedding is called a *polyhedral graph*.

A *knot* is an embedding of a circle in three dimensional space \mathbb{R}^3 . A *link* L is a collection of knots which may be linked or knotted together without intersections. Each knot is called a *component* of L . A *knot* is considered as a link with one component. The link L can be oriented by giving one of the two directions along each component. L with the opposite orientation, denoted by $-L$, is called *the reverse of L* . The mirror image of L is denoted by L^* and the link $-L^*$ is called *the inverse of L* . A *link diagram* is a regular

projection of a link onto a plane such that the corresponding space curve crosses over or under at each crossing is indicated by creating broken strands.

Two links L_1 and L_2 are *equivalent*, denoted by $L_1 = L_2$, if there exists an ambient isotopy that maps one to the other. An oriented link L is called *achiral link* if it is equivalent to its mirror image L^* . Otherwise, it is called *chiral*. It is well-known that ambient isotopy is an equivalence relation on links. Each equivalence class of links is called a link type, and the link type of a link diagram means the equivalence class of the link represented by this diagram. Here two links are considered to be the same if they are equivalent (or belong to the same link type). Otherwise, they are considered different. With some abuse of terminology, the word ‘link’ is applied to mean a whole equivalence class (a knot type) or a particular representative member.

2.2 The construction of tetrahedral links

A *twist tangle* of length m , denoted by T , is two parallel strands with m half-twists for any positive integer m . Four endpoints of T are marked by NW , NE , SW and SE , as shown in Fig.1(a). There are four possible ways to twist two strands of T , hence we have four types of twist tangles denoted by a_m , b_m , a_m^* and b_m^* . Note that a_m^* and b_m^* are the mirror images of a_m and b_m respectively, hence we only consider the tangles a_m and b_m as building blocks to obtain alternating links.

A twist tangle can be oriented by assigning a direction to its each strand. Then T allow three possible orientations α , β , γ and their reverse orientations $-\alpha$, $-\beta$ and $-\gamma$, as shown in Fig. 1(b). Note that the orientation $-\beta$ (or $-\gamma$) overlaps the orientation β (or γ) for T by rotating it by 180 degrees in the plane. Hence we only need to consider the orientations α , β , γ and $-\alpha$ for T .

We note that the twist tangles a_m and b_m can be oriented respectively with α and $-\alpha$ when $m = 2n$ ($n \in \mathbb{Z}^+$). The twist tangles a_m can be oriented with β and b_m can be oriented with γ when $m = 2n - 1$ ($n \in \mathbb{Z}^+$). As a result, we obtain six types of oriented twist tangles, denoted by a_{2n}^α , $a_{2n}^{-\alpha}$, a_{2n-1}^β , b_{2n}^α , $b_{2n}^{-\alpha}$ and b_{2n-1}^γ , such that each type has an antiparallel orientation on its two strands (Fig. 1(c)). Here the twist tangle $a_{2n}^{-\alpha}$ (or $b_{2n}^{-\alpha}$) can be obtained from a_{2n}^α (or b_{2n}^α) by reversing the orientations on two strands. In fact, any other oriented twist tangle with such antiparallel orientation must be one of the mirror images of the above six types.

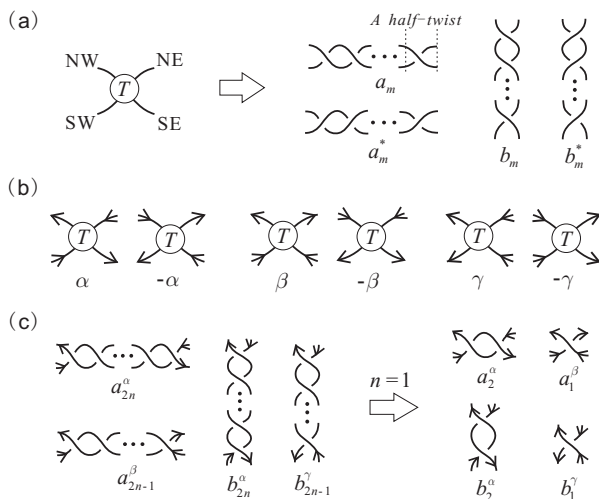


Figure 1. (a) Four types of twist tangles: a_m , a_m^* , b_m and b_m^* ; (b) Six orientations: α , β , γ , $-\alpha$, $-\beta$ and $-\gamma$; (c) Four types of oriented twist tangles: a_{2n}^α , a_{2n-1}^β , b_{2n}^α and b_{2n-1}^γ .

Given a tetrahedral graph G , each edge e_i is replaced by an oriented twist tangle T_i , where T_i is one of the above six types of oriented twist tangles for $1 \leq i \leq 6$ (Fig. 2). And then we connect the endpoints of two twist tangles along the boundary of each face. As a result, an oriented tetrahedral link diagram $D(G)$, called an *OT-link diagram*, is obtained. Clearly, $D(G)$ is alternating. For convenience, $D(G)$ is also denoted as $D(T_1, T_2, T_3, T_4, T_5, T_6)$ by recording the twist tangle on each edge in a sequence from left to right and top to bottom. Also, the orientation of $D(G)$ is denoted as $o(\tau_1, \tau_2, \tau_3, \tau_4, \tau_5, \tau_6)$, where τ_i is the orientation of T_i for $1 \leq i \leq 6$. Here there exists only one oriented tetrahedral link in \mathbb{R}^3 , denoted by $L(T_1, T_2, T_3, T_4, T_5, T_6)$, corresponding to the diagram $D(G)$ such that $D(G)$ is a spherical embedding of $L(T_1, T_2, T_3, T_4, T_5, T_6)$. In Fig. 2, we take the diagram $D(b_2^\alpha, 3a_1^\beta, a_2^{-\alpha}, a_1^\beta)$ for an example and give the corresponding link $L(b_2^\alpha, 3a_1^\beta, a_2^{-\alpha}, a_1^\beta)$.

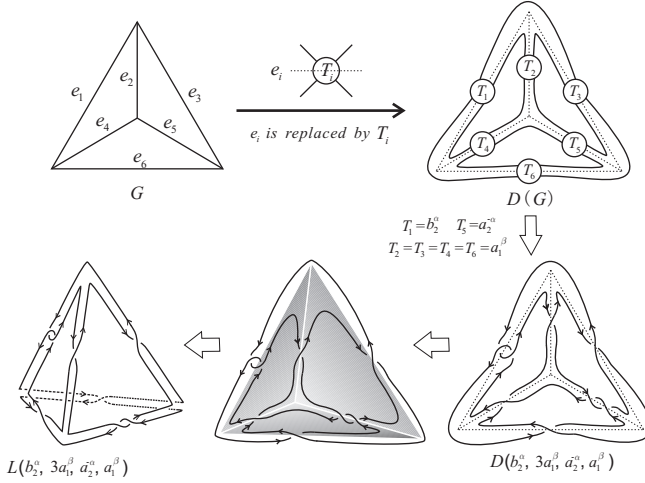


Figure 2. The construction of $D(G)$, $D(b_2^\alpha, 3a_1^\beta, a_2^{-\alpha}, a_1^\beta)$ and $L(b_2^\alpha, 3a_1^\beta, a_2^{-\alpha}, a_1^\beta)$.

In the above construction process, we must avoid the conflict orientations for any two oriented twist tangles whose endpoints are connected. The following theorem provides an approach to giving all OT-link diagrams.

Theorem 2.1. *Let G be a tetrahedral graph. Then there are 27 link types of OT-link diagrams constructed from G , as listed in Table 1.*

D	$c(D)$	$\mu(D)$	$w(D)$	c or ac	D^*
$D(6b_{2n}^\alpha)$	12n	4	12n	c	$D(6a_{2n}^\alpha)$
$D(a_{2n}^\alpha, 5b_{2n}^\alpha)$		3	8n	c	$D(b_{2n}^\alpha, 5a_{2n}^\alpha)$
$D(2a_{2n}^\alpha, 4b_{2n}^\alpha)$		2	4n	c	$D(2b_{2n}^\alpha, 4a_{2n}^\alpha)$
$D(a_{2n}^\alpha, 3b_{2n}^\alpha, a_{2n}^\alpha, b_{2n}^\alpha)$		2	4n	c	$D(b_{2n}^\alpha, 3a_{2n}^\alpha, b_{2n}^\alpha, a_{2n}^\alpha)$
$D(3b_{2n}^\alpha, 3a_{2n}^\alpha)$		3	0	ac	
$D(3a_{2n}^\alpha, 3b_{2n}^\alpha)$		1	0	ac	
$D(a_{2n}^\alpha, 3b_{2n}^\alpha, 2a_{2n}^\alpha)$		1	0	ac	$D(2a_{2n}^\alpha, 3b_{2n}^\alpha, a_{2n}^\alpha)$
$D(3b_{2n}^\alpha, 3b_{2n-1}^\alpha)$	12n-3	2	12n-3	c	$D(a_{2n}^\alpha, a_{2n-1}^\alpha, a_{2n}^\alpha, 2a_{2n-1}^\alpha, a_{2n}^\alpha)$
$D(2a_{2n}^\alpha, b_{2n}^\alpha, 3b_{2n-1}^\alpha)$		2	4n-3	c	$D(b_{2n}^\alpha, a_{2n-1}^\alpha, b_{2n}^\alpha, 2a_{2n-1}^\alpha, a_{2n}^\alpha)$
$D(a_{2n}^\alpha, 2b_{2n}^\alpha, 3b_{2n-1}^\alpha)$		1	8n-3	c	$D(a_{2n}^\alpha, a_{2n-1}^\alpha, b_{2n}^\alpha, 2a_{2n-1}^\alpha, a_{2n}^\alpha)$
$D(3a_{2n}^\alpha, 3b_{2n-1}^\alpha)$		1	-3	c	$D(b_{2n}^\alpha, a_{2n-1}^\alpha, b_{2n}^\alpha, 2a_{2n-1}^\alpha, b_{2n}^\alpha)$
$D(b_{2n}^\alpha, 3b_{2n-1}^\alpha, a_{2n}^{-\alpha}, b_{2n-1}^\alpha)$	12n-4	3	8n-4	c	$D(a_{2n}^\alpha, 3a_{2n-1}^\beta, b_{2n}^{-\alpha}, a_{2n}^\alpha)$
$D(b_{2n}^\alpha, 3b_{2n-1}^\alpha, b_{2n}^{-\alpha}, b_{2n-1}^\alpha)$		2	12n-4	c	$D(a_{2n}^\alpha, 3a_{2n-1}^\beta, a_{2n}^{-\alpha}, a_{2n}^\alpha)$
$D(a_{2n}^\alpha, 3b_{2n-1}^\alpha, a_{2n}^{-\alpha}, b_{2n-1}^\alpha)$		2	4n-4	c	$D(b_{2n}^\alpha, 3a_{2n-1}^\beta, b_{2n}^{-\alpha}, a_{2n}^\alpha)$
$D(2b_{2n-1}^\alpha, a_{2n-1}^\alpha, b_{2n-1}^\alpha, 2a_{2n-1}^\alpha)$	12n-6	3	0	ac	

Table 1. The invariants of any OT-link diagram D (Here ‘c’ and ‘ac’ mean chirality and achirality respectively).

Proof: First, each edge of G is labeled with e_i for $1 \leq i \leq 6$, as shown in Fig. 2. Let $D(G)$ be an OT-link diagram obtained from G by replacing each edge e_i with an oriented twist tangle T_i with the orientation τ_i ($1 \leq i \leq 6$).

Claim 1. The OT-link diagram $D(G)$ only possibly allow these six orientations $o(6\alpha)$, $o(3\alpha, 3\gamma)$, $o(\alpha, \beta, \alpha, 2\beta, \alpha)$, $o(\alpha, 3\gamma, -\alpha, \gamma)$, $o(\alpha, 3\beta, -\alpha, \beta)$, $o(2\gamma, \beta, \gamma, 2\beta)$ or their reverses.

Proof: Without loss of generality, $D(G)$ is oriented starting from the twist edge T_1 . Hence there are two cases we need to consider according to the orientation of $D(G)$.

Case 1. Assume that in $D(G)$, there is no twist tangle with the orientation α . If $D(G)$ has an twist tangle with the orientation γ , without loss of generality, we can assume that this twist tangle is T_1 . Then its adjacent twist tangle T_2 only possibly has the orientations γ and β (Fig. 3(a)). Once the orientation of T_2 is given, the orientations of the remaining twist tangles for $D(G)$ will be determined. Thus, in this case, two orientations $o(2\gamma, \beta, \gamma, 2\beta)$ and $o(\gamma, \beta, \gamma, 2\beta, \gamma)$ can be obtained for $D(G)$.

If $D(G)$ has no twist tangle with the orientation γ , each twist tangle of $D(G)$ will be oriented with β . It doesn't happen in this case due to the conflict orientation produced by two adjacent twist tangles for $D(G)$.

Case 2. Assume that in $D(G)$, there is at least an twist tangle with the orientation α . If $D(G)$ has a twist tangle with the orientation α , without loss of generality, we can assume that this twist tangle is T_1 . Then its adjacent twist tangle T_2 has three possible orientations α , β and γ shown in Fig. 3(b). When the twist tangle T_2 is oriented with α , the adjacent twist tangle T_3 will be possibly oriented with α and β respectively. At last, three orientations $o(6\alpha)$, $o(3\alpha, 3\gamma)$ and $o(2\alpha, \beta, \alpha, 2\beta)$ of $D(G)$ are obtained.

Similarly, when the twist tangle T_2 is oriented with β , the orientations $o(\alpha, \beta, \alpha, 2\beta, \alpha)$ and $o(\alpha, 3\beta, -\alpha, \beta)$ of $D(G)$ are obtained. When T_1 is oriented with γ , the orientations $o(\alpha, 2\gamma, \alpha, \gamma, \alpha)$ and $o(\alpha, 3\gamma, -\alpha, \gamma)$ of $D(G)$ are obtained (Fig. 3(b)).

At last, we can obtain nine orientations of $D(G)$, that are $o(2\gamma, \beta, \gamma, 2\beta)$, $o(\gamma, \beta, \gamma, 2\beta, \gamma)$, $o(6\alpha)$, $o(3\alpha, 3\gamma)$, $o(2\alpha, \beta, \alpha, 2\beta)$, $o(\alpha, 2\gamma, \alpha, \gamma, \alpha)$, $o(\alpha, 3\gamma, -\alpha, \gamma)$, $o(\alpha, \beta, \alpha, 2\beta, \alpha)$ and $o(\alpha, 3\beta, -\alpha, \beta)$. Note that the orientation $o(3\alpha, 3\gamma)$ is the same as the orientation $o(\alpha, 2\gamma, \alpha, \gamma, \alpha)$ for $D(G)$. Moreover, when $D(G)$ is embedded into \mathbb{R}^3 as an oriented link $L(G)$, the orientation $o(2\alpha, \beta, \alpha, 2\beta)$ overlaps the orientation $o(\alpha, \beta, \alpha, 2\beta, \alpha)$, and $o(2\gamma, \beta, \gamma, 2\beta)$ is the reverse orientation of $o(\gamma, \beta, \gamma, 2\beta, \gamma)$. Then we only need to consider the following six orientations, that are $o(6\alpha)$, $o(3\alpha, 3\gamma)$, $o(\alpha, \beta, \alpha, 2\beta, \alpha)$, $o(\alpha, 3\gamma, -\alpha, \gamma)$, $o(\alpha, 3\beta, -\alpha, \beta)$

and $o(2\gamma, \beta, \gamma, 2\beta)$. Hence the OT-link diagram $D(G)$ only possibly allow the above six orientations or their reverses. ■

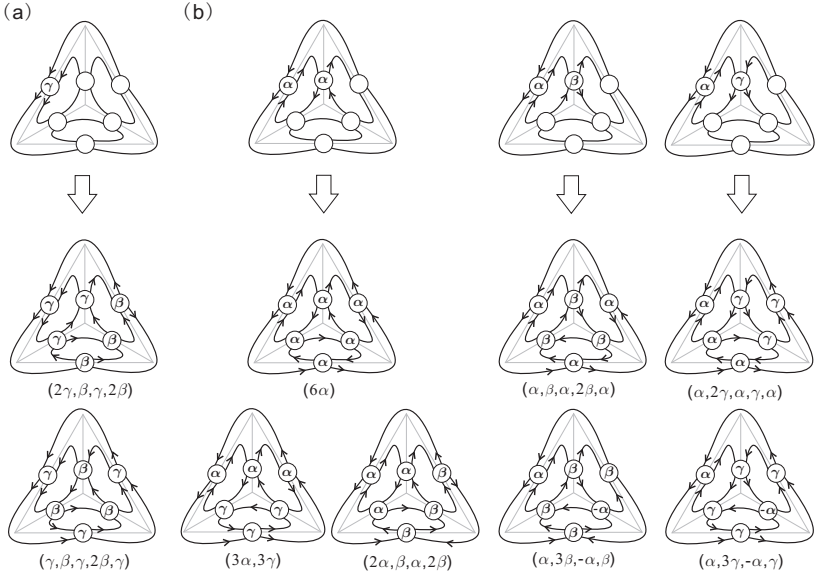


Figure 3. (a) There are two orientations for $D(G)$ in case 1; (b) There are seven orientations in case 2.

All OT-link diagrams will be constructed by using the above six orientations as below. First, for the orientation $o(2\gamma, \beta, \gamma, 2\beta)$ of $D(G)$, the twist tangles oriented with β (or γ) must be a_{2n-1}^β (or b_{2n-1}^γ), hence we obtain an OT-link diagram $D(2b_{2n-1}^\gamma, a_{2n-1}^\beta, b_{2n-1}^\gamma, 2a_{2n-1}^\beta)$.

For the orientation $o(6\alpha)$, each twist tangle with the orientation α must be a_{2n}^α or b_{2n}^α , thus the number of the resulting OT-link diagrams can be calculated by the following formula

$$2C_6^0 + 2C_6^1 + 2C_6^2 + C_6^3 = 64.$$

Among these link diagrams, many of them are equivalent since they are corresponding to the same link in \mathbb{R}^3 . First, when all twist tangles of $D(G)$ are all a_{2n}^α or all b_{2n}^α , we will obtain the OT-link diagram $D(6a_{2n}^\alpha)$ or $D(6b_{2n}^\alpha)$. When a twist tangle is b_{2n}^α and the remaining edges are all a_{2n}^α , we will obtain OT-link diagrams of C_6^1 , that are $D(b_{2n}^\alpha, 5a_{2n}^\alpha)$, $D(a_{2n}^\alpha, b_{2n}^\alpha, 4a_{2n}^\alpha)$, $D(2a_{2n}^\alpha, b_{2n}^\alpha, 3a_{2n}^\alpha)$, $D(3a_{2n}^\alpha, b_{2n}^\alpha, 2a_{2n}^\alpha)$, $D(4a_{2n}^\alpha, b_{2n}^\alpha, a_{2n}^\alpha)$ and

$D(5a_{2n}^\alpha, b_{2n}^\alpha)$. Since these six link diagrams are corresponding to the same OT-link in \mathbb{R}^3 , we use $D(b_{2n}^\alpha, 5a_{2n}^\alpha)$ to represent this link type. Similarly, when a twist tangle is a_{2n}^α and the remaining tangles are all b_{2n}^α in $D(G)$, we will obtain the OT-link diagram $D(a_{2n}^\alpha, 5b_{2n}^\alpha)$.

Furthermore, when two twist tangles are both of a_{2n}^α and the remaining twist tangles are all b_{2n}^α in $D(G)$, we will obtain OT-link diagrams of C_6^2 . These diagrams can be divided into two classes such that, in each class, all diagrams are corresponding to the same link in \mathbb{R}^3 . One class has three OT-link diagrams $D(b_{2n}^\alpha, 3a_{2n}^\alpha, b_{2n}^\alpha, a_{2n}^\alpha)$, $D(a_{2n}^\alpha, b_{2n}^\alpha, 3a_{2n}^\alpha, b_{2n}^\alpha)$ and $D(2a_{2n}^\alpha, 2b_{2n}^\alpha, 2a_{2n}^\alpha)$, where two a_{2n}^α aren't adjacent in each link diagram. The remaining link diagrams consist of the other class, including $D(2b_{2n}^\alpha, 4a_{2n}^\alpha)$, $D(a_{2n}^\alpha, 2b_{2n}^\alpha, 3a_{2n}^\alpha)$, $D(2a_{2n}^\alpha, b_{2n}^\alpha, a_{2n}^\alpha, b_{2n}^\alpha, a_{2n}^\alpha)$, $D(3a_{2n}^\alpha, 2b_{2n}^\alpha, a_{2n}^\alpha)$, $D(4a_{2n}^\alpha, 2b_{2n}^\alpha)$, $D(b_{2n}^\alpha, a_{2n}^\alpha, b_{2n}^\alpha, 3a_{2n}^\alpha)$, $D(b_{2n}^\alpha, 2a_{2n}^\alpha, b_{2n}^\alpha, 2a_{2n}^\alpha)$, $D(a_{2n}^\alpha, b_{2n}^\alpha, a_{2n}^\alpha, b_{2n}^\alpha, 2a_{2n}^\alpha)$, $D(b_{2n}^\alpha, 4a_{2n}^\alpha, b_{2n}^\alpha)$, $D(2a_{2n}^\alpha, b_{2n}^\alpha, 2a_{2n}^\alpha, b_{2n}^\alpha)$, $D(3a_{2n}^\alpha, b_{2n}^\alpha, a_{2n}^\alpha, b_{2n}^\alpha)$ and $D(4a_{2n}^\alpha, 2b_{2n}^\alpha)$. Here we use the diagrams $D(2b_{2n}^\alpha, 4a_{2n}^\alpha)$ and $D(b_{2n}^\alpha, 3a_{2n}^\alpha, b_{2n}^\alpha, a_{2n}^\alpha)$ to represent the above two link types respectively. Similarly, when two twist tangles are both of b_{2n}^α and the remaining four edges are all a_{2n}^α in $D(G)$, we will obtain the OT-link diagrams $D(a_{2n}^\alpha, 3b_{2n}^\alpha, a_{2n}^\alpha, b_{2n}^\alpha)$ and $D(2a_{2n}^\alpha, 4b_{2n}^\alpha)$.

At last, in $D(G)$ when three edges are all a_{2n}^α and the remaining three edges are all b_{2n}^α , we obtain OT-link diagrams of C_6^3 in total. These diagrams are divided into four classes such that, in each class, all diagrams are corresponding to the same link in \mathbb{R}^3 . In the first class, for each diagram, three a_{2n}^α forms a face of $D(G)$, which includes four members $D(3b_{2n}^\alpha, 3a_{2n}^\alpha)$, $D(b_{2n}^\alpha, 2a_{2n}^\alpha, b_{2n}^\alpha, a_{2n}^\alpha, b_{2n}^\alpha)$, $D(a_{2n}^\alpha, b_{2n}^\alpha, a_{2n}^\alpha, 2b_{2n}^\alpha, a_{2n}^\alpha)$ and $D(2a_{2n}^\alpha, b_{2n}^\alpha, a_{2n}^\alpha, 2b_{2n}^\alpha)$. In the second class, for each diagram, three b_{2n}^α forms a face of $D(G)$, which includes four members $D(3a_{2n}^\alpha, 3b_{2n}^\alpha)$, $D(2b_{2n}^\alpha, a_{2n}^\alpha, b_{2n}^\alpha, 2a_{2n}^\alpha)$, $D(b_{2n}^\alpha, a_{2n}^\alpha, b_{2n}^\alpha, 2a_{2n}^\alpha, b_{2n}^\alpha)$ and $D(a_{2n}^\alpha, 2b_{2n}^\alpha, a_{2n}^\alpha, b_{2n}^\alpha, a_{2n}^\alpha)$. The third class includes $D(a_{2n}^\alpha, 3b_{2n}^\alpha, 2a_{2n}^\alpha)$, $D(2b_{2n}^\alpha, 3a_{2n}^\alpha, b_{2n}^\alpha)$, $D(b_{2n}^\alpha, 2a_{2n}^\alpha, 2b_{2n}^\alpha, a_{2n}^\alpha)$, $D(b_{2n}^\alpha, a_{2n}^\alpha, b_{2n}^\alpha, a_{2n}^\alpha, b_{2n}^\alpha, a_{2n}^\alpha)$, $D(a_{2n}^\alpha, b_{2n}^\alpha, 2a_{2n}^\alpha, 2b_{2n}^\alpha)$ and $D(2a_{2n}^\alpha, 2b_{2n}^\alpha, a_{2n}^\alpha, b_{2n}^\alpha)$. The remaining links consists of the fourth class, that are $D(2a_{2n}^\alpha, 3b_{2n}^\alpha, a_{2n}^\alpha)$, $D(b_{2n}^\alpha, 3a_{2n}^\alpha, 2b_{2n}^\alpha)$, $D(2b_{2n}^\alpha, 2a_{2n}^\alpha, b_{2n}^\alpha, a_{2n}^\alpha)$, $D(b_{2n}^\alpha, a_{2n}^\alpha, 2b_{2n}^\alpha, 2a_{2n}^\alpha)$, $D(a_{2n}^\alpha, 2b_{2n}^\alpha, 2a_{2n}^\alpha, b_{2n}^\alpha)$ and $D(a_{2n}^\alpha, b_{2n}^\alpha, a_{2n}^\alpha, b_{2n}^\alpha, a_{2n}^\alpha, b_{2n}^\alpha)$. We use the diagrams $D(3b_{2n}^\alpha, 3a_{2n}^\alpha)$, $D(3a_{2n}^\alpha, 3b_{2n}^\alpha)$, $D(a_{2n}^\alpha, 3b_{2n}^\alpha, 2a_{2n}^\alpha)$ and $D(2a_{2n}^\alpha, 3b_{2n}^\alpha, a_{2n}^\alpha)$ to represent the above four link types respectively.

For the orientation $o(3\alpha, 3\gamma)$ for $D(G)$, three twist tangles with the orientation γ are all b_{2n-1}^γ , then the number of the obtaining OT-link diagrams is calculated as follows

$$C_3^0 + C_3^1 + C_3^2 + C_3^3 = 8.$$

When there is only one twist tangle a_{2n}^α in $D(G)$, we obtain three OT-link dia-

grams $(2b_{2n}^\alpha, a_{2n}^\alpha, 3b_{2n-1}^\gamma)$, $D(b_{2n}^\alpha, a_{2n}^\alpha, b_{2n}^\alpha, 3b_{2n-1}^\gamma)$ and $D(a_{2n}^\alpha, 2b_{2n}^\alpha, 3b_{2n-1}^\gamma)$. They are all equivalent since they are corresponding to the same link in \mathbb{R}^3 . We use the diagram $D(a_{2n}^\alpha, 2b_{2n}^\alpha, 3b_{2n-1}^\gamma)$ to represent this link type. Similarly, when there are only two a_{2n}^α in $D(G)$, we will obtain the diagram $(2a_{2n}^\alpha, b_{2n}^\alpha, 3b_{2n-1}^\gamma)$. When there are three a_{2n}^α in $D(G)$, we will obtain the OT-link diagrams $(3a_{2n}^\alpha, 3b_{2n-1}^\gamma)$ and $(3b_{2n}^\alpha, 3b_{2n-1}^\gamma)$. At last, we obtain four link types of OT-link diagrams, that are $(3a_{2n}^\alpha, 3b_{2n-1}^\gamma)$, $(3b_{2n}^\alpha, 3b_{2n-1}^\gamma)$, $(2a_{2n}^\alpha, b_{2n}^\alpha, 3b_{2n-1}^\gamma)$ and $D(a_{2n}^\alpha, 2b_{2n}^\alpha, 3b_{2n-1}^\gamma)$. Similarly for the orientation $(\alpha, \beta, \alpha, 2\beta, \alpha)$, we also obtain four link types of OT-link diagrams $D(a_{2n}^\alpha, a_{2n-1}^\beta, a_{2n}^\alpha, 2a_{2n-1}^\beta, a_{2n}^\alpha)$, $D(b_{2n}^\alpha, a_{2n-1}^\beta, b_{2n}^\alpha, 2a_{2n-1}^\beta, b_{2n}^\alpha)$, $D(a_{2n}^\alpha, a_{2n-1}^\beta, b_{2n}^\alpha, 2a_{2n-1}^\beta, a_{2n}^\alpha)$ and $D(b_{2n}^\alpha, b_{2n}^\alpha, 2a_{2n-1}^\beta, a_{2n}^\alpha, a_{2n-1}^\beta)$.

For the orientation $o(\alpha, 3\gamma, -\alpha, \gamma)$ of $D(G)$, four twist tangles with the orientation γ are all a_{2n-1}^β . Also, the twist tangle oriented with $-\alpha$ will be $a_{2n}^{-\alpha}$ or $b_{2n}^{-\alpha}$. Hence there will be four OT-link diagrams with the orientation $o(\alpha, 3\gamma, -\alpha, \gamma)$, that are $D(a_{2n}^\alpha, 3b_{2n-1}^\gamma, a_{2n}^{-\alpha}, b_{2n-1}^\gamma)$, $D(b_{2n}^\alpha, 3b_{2n-1}^\gamma, b_{2n}^{-\alpha}, b_{2n-1}^\gamma)$, $D(b_{2n}^\alpha, 3b_{2n-1}^\gamma, a_{2n}^{-\alpha}, b_{2n-1}^\gamma)$ and $D(a_{2n}^\alpha, 3b_{2n-1}^\gamma, b_{2n}^{-\alpha}, b_{2n-1}^\gamma)$. Note that the last two diagrams have reverse orientations as the the same link in \mathbb{R}^3 . Here we don't distinguish these two link diagrams and only consider the diagram $D(b_{2n}^\alpha, 3b_{2n-1}^\gamma, a_{2n}^{-\alpha}, b_{2n-1}^\gamma)$. At last, we obtain three link types of OT-link diagrams, that are $D(a_{2n}^\alpha, 3b_{2n-1}^\gamma, a_{2n}^{-\alpha}, b_{2n-1}^\gamma)$, $D(b_{2n}^\alpha, 3b_{2n-1}^\gamma, a_{2n}^{-\alpha}, b_{2n-1}^\gamma)$ and $D(b_{2n}^\alpha, 3b_{2n-1}^\gamma, b_{2n}^{-\alpha}, b_{2n-1}^\gamma)$. Similarly, for the orientation $o(\alpha, 3\beta, -\alpha, \beta)$, we also obtain three link types of OT-link diagrams, that are $D(a_{2n}^\alpha, 3a_{2n-1}^\beta, a_{2n}^{-\alpha}, a_{2n-1}^\beta)$, $D(a_{2n}^\alpha, 3a_{2n-1}^\beta, b_{2n}^{-\alpha}, a_{2n-1}^\beta)$ and $D(b_{2n}^\alpha, 3a_{2n-1}^\beta, b_{2n}^{-\alpha}, a_{2n-1}^\beta)$.

At last, we obtain 27 link types of OT-link diagrams. Also, by the above construction process, each OT-link diagram must be one of these 27 link types or one of their reverse. Thus we complete the proof for this theorem. ■

In the following two sections, we will show that the 27 link types of OT-link diagrams contains a mirror pair of the achiral links $(D(a_{2n}^\alpha, 3b_{2n}^\alpha, 2a_{2n}^\alpha)$ and $D(2a_{2n}^\alpha, 3b_{2n}^\alpha, a_{2n}^\alpha)$), and hence further show that there are exactly 26 different link types for OT-link diagrams.

3 Results

3.1 Duality of OT-link diagrams

In graph theory, the dual graph G^d of a plane graph G is a plane graph whose vertices correspond to the faces of G . The edges of G^d corresponding to the edges of G as follows: If e is an edge of G with face X on one side and face Y on the other side, then the

endpoints of the dual edge e^d are the vertices x, y of G^d that represent the faces X, Y of G . Note that any polyhedral graph has a unique dual graph [51]. In particular, the dual graph G^d of a tetrahedral graph G is still a tetrahedral graph (Fig. 4(a)).

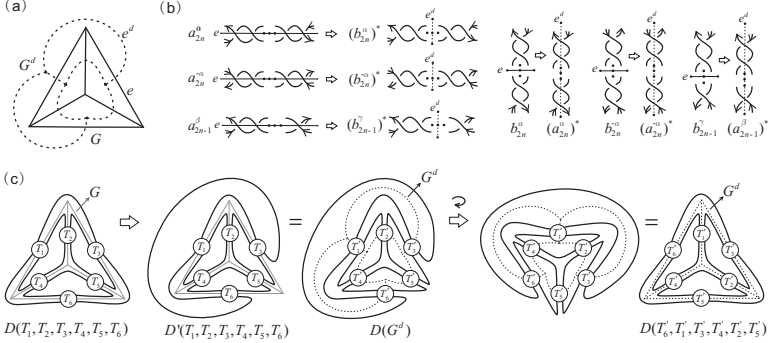


Figure 4. (a) Tetrahedral graph G and its dual graph G^d . (b) The twist tangles $(b_{2n}^\alpha)^*$, $(b_{2n}^{-\alpha})^*$, $(b_{2n-1}^\gamma)^*$, $(a_{2n}^\alpha)^*$, $(a_{2n}^{-\alpha})^*$ and $(a_{2n-1}^\beta)^*$ used to replace the dual edge e^d . (c) $D(T_1, T_2, T_3, T_4, T_5, T_6)$ is transformed equivalently to $D(T'_6, T'_1, T'_3, T'_4, T'_2, T'_5)$.

Let $D(G)$ and G be defined as in Fig. 4(a). Hereafter we use $(\sim)^*$ to denote the mirror image of a twist tangle \sim . An link diagram $D(G^d)$ can be constructed from G^d such that each edge e^d is replaced by the twist tangles $(b_{2n}^\alpha)^*$, $(b_{2n}^{-\alpha})^*$, $(a_{2n}^\alpha)^*$, $(a_{2n}^{-\alpha})^*$, $(b_{2n-1}^\gamma)^*$ or $(a_{2n-1}^\beta)^*$ if the related edge e of G is replaced accordingly by a_{2n}^α , $a_{2n}^{-\alpha}$, b_{2n}^α , $b_{2n}^{-\alpha}$, a_{2n-1}^β or b_{2n-1}^γ (Fig. 4(b)). This diagram $D(G^d)$ is called the dual link diagram of $D(G)$. In fact, according to the construction method of $D(G^d)$, we have the following theorem.

Theorem 3.1. *The OT-link diagrams $D(G)$ and its dual link diagram $D(G^d)$ are ambient isotopic.*

Proof: Let $D(G)$ be described as the link diagram $D(T_1, T_2, T_3, T_4, T_5, T_6)$ in Fig. 4(c), where T_i is the oriented twist tangle a_{2n}^α , $a_{2n}^{-\alpha}$, b_{2n}^α , $b_{2n}^{-\alpha}$, a_{2n-1}^β or b_{2n-1}^γ .

First, $D(T_1, T_2, T_3, T_4, T_5, T_6)$ is transformed into the link diagram $D'(T_1, T_2, T_3, T_4, T_5, T_6)$ by using a series of Reidemeister moves, as illustrated in Fig. 4(c). Hence $D(T_1, T_2, T_3, T_4, T_5, T_6)$ and $D'(T_1, T_2, T_3, T_4, T_5, T_6)$ are equivalent.

For $D'(T_1, T_2, T_3, T_4, T_5, T_6)$, the underlying graph G is replaced by the corresponding dual graph G^d . Then each twist tangle T_i corresponding to the original edge e_i is corresponding to the edge e_i^d , that is exactly the mirror image $(T_i')^* = T_i'$ of some twist

tangle $T_{i'}$ ($1 \leq i' \leq 6$) according to the relations described in Fig. 4(b). According to this construction method, $D'(T_1, T_2, T_3, T_4, T_5, T_6)$ corresponding to G^d is exactly the dual link diagram $D(G^d)$ of $D(G)$. Then we have

$$D(G) = D'(T_1, T_2, T_3, T_4, T_5, T_6) = D(G^d).$$

In addition, $D(G^d)$ is rotated 60 degrees clockwise in the plane, and then is stretched to obtain the link diagram $D(T'_6, T'_1, T'_3, T'_4, T'_2, T'_5)$ in Fig. 4(c). Hence $D(G^d)$ is ambient isotopic to $D(T'_6, T'_1, T'_3, T'_4, T'_2, T'_5)$. Then we have

$$D(G) = D(T_1, T_2, T_3, T_4, T_5, T_6) = D(G^d) = D(T'_6, T'_1, T'_3, T'_4, T'_2, T'_5).$$

We finished the proof of this theorem. ■

By using the above theorem, we obtain the following results.

Theorem 3.2. *The OT-link diagrams $D(3b_{2n}^\alpha, 3a_{2n}^\alpha)$, $D(3a_{2n}^\alpha, 3b_{2n}^\alpha)$, $D(a_{2n}^\alpha, 3b_{2n}^\alpha, 2a_{2n}^\alpha)$ and $D(2b_{2n-1}^\gamma, a_{2n-1}^\beta, b_{2n-1}^\gamma, 2a_{2n-1}^\beta)$ are all achiral.*

Proof: First, the OT-link diagram $D(3a_{2n}^\alpha, 3b_{2n}^\alpha)$ is equivalent to the link diagram $D((a_{2n}^\alpha)^*, 2(b_{2n}^\alpha)^*, (a_{2n}^\alpha)^*, (b_{2n}^\alpha)^*, (a_{2n}^\alpha)^*)$ according to the proof of theorem 3.1. On the other hand, $D((a_{2n}^\alpha)^*, 2(b_{2n}^\alpha)^*, (a_{2n}^\alpha)^*, (b_{2n}^\alpha)^*, (a_{2n}^\alpha)^*)$ can overlap the link diagram $D^*(3a_{2n}^\alpha, 3b_{2n}^\alpha)$ by rotating it 120 degrees clockwise. Then $D(3a_{2n}^\alpha, 3b_{2n}^\alpha)$ and $D^*(3a_{2n}^\alpha, 3b_{2n}^\alpha)$ are equivalent. Hence the link diagram $D(3a_{2n}^\alpha, 3b_{2n}^\alpha)$ is achiral. Similarly, the link diagram $D(3b_{2n}^\alpha, 3a_{2n}^\alpha)$ can be proved to be achiral in the same way.

For the link diagram $D(a_{2n}^\alpha, 3b_{2n}^\alpha, 2a_{2n}^\alpha)$, it is equivalent to the link diagram $D(2(b_{2n}^\alpha)^*, 3(a_{2n}^\alpha)^*, (b_{2n}^\alpha)^*)$ by using theorem 3.1. Also, $D(2(b_{2n}^\alpha)^*, 3(a_{2n}^\alpha)^*, (b_{2n}^\alpha)^*)$ and $D^*(a_{2n}^\alpha, 3b_{2n}^\alpha, 2a_{2n}^\alpha)$ are corresponding to the same link in \mathbb{R}^3 . Then $D(b_{2n}^\alpha, 3a_{2n}^\alpha, 2b_{2n}^\alpha)$ and $D^*(a_{2n}^\alpha, 3b_{2n}^\alpha, 2a_{2n}^\alpha)$ are equivalent. Hence $D(a_{2n}^\alpha, 3b_{2n}^\alpha, 2a_{2n}^\alpha)$ is achiral. Similarly, the link diagram $D(2a_{2n-1}^\beta, b_{2n-1}^\gamma, a_{2n-1}^\beta, b_{2n-1}^\gamma)$ can be proved to be achiral in the same way. ■

Note. In table 1, 27 link types of OT-link diagrams includes 11 mirror-image pairs according to the theorem 3.1.

3.2 Crossing number and writhe number of OT-link diagrams

The crossing number of a link L is the minimum number of crossings in any diagram D of L , and is denoted by $c(L)$. It is well-known that the number of crossings in a reduced alternating link diagram of L is a topological invariant of L . For any link diagram D , each

crossing is given a sign of plus 1 or minus 1 according to the conventions shown in Fig. 5. The twist number $w(D)$ of D is the sum of the signs of all the crossings, that is the simplest invariant of regular isotopy for oriented link diagrams. In 1989, Kauffman [47] give this association among crossing number, twist number and chirality for a link diagram, which is described as below:

Lemma 3.3. *Let D be a simple alternating diagram which is not the unknotted circle diagram, and $T(D) = |w(D)|$. If $T(D) \geq \frac{c(D)}{3}$, then D is chiral.*

Clearly, each OT-link diagram is simple, alternating and nontrivial, hence we obtain the following theorem.

Theorem 3.4. *The OT-link diagrams $(6b_{2n}^\alpha)$, $(a_{2n}^\alpha, 5b_{2n}^\alpha)$, $(2a_{2n}^\alpha, 4b_{2n}^\alpha)$, $D(3b_{2n}^\alpha, 3b_{2n-1}^\gamma)$, $(a_{2n}^\alpha, 3b_{2n}^\alpha, a_{2n}^\alpha, b_{2n}^\alpha)$, $(a_{2n}^\alpha, 2b_{2n}^\alpha, 3b_{2n-1}^\gamma)$, $(b_{2n}^\alpha, 3b_{2n-1}^\gamma, a_{2n}^{-\alpha}, b_{2n-1}^\gamma)$ and $(b_{2n}^\alpha, 3b_{2n-1}^\gamma, b_{2n}^{-\alpha}, b_{2n-1}^\gamma)$ are all chiral.*

Proof: Note that the twist tangles a_{2n}^α , $a_{2n}^{-\alpha}$ and a_{2n-1}^β only have negative sign for each crossing while the twist tangles b_{2n}^α , $b_{2n}^{-\alpha}$ and b_{2n-1}^γ only have positive sign for each crossing. Let x_α , $x_{-\alpha}$, x_β , y_α , $y_{-\alpha}$ and y_γ be the number of the twist tangles a_{2n}^α , $a_{2n}^{-\alpha}$, a_{2n-1}^β , b_{2n}^α , $b_{2n}^{-\alpha}$ and b_{2n-1}^γ in the OT-link diagram $D(G)$ respectively. Hence we have

$$\begin{aligned} w(D(G)) = & (-1) \cdot 2n \cdot (x_\alpha + x_{-\alpha}) + (-1) \cdot (2n - 1) \cdot x_\beta \\ & + 2n \cdot (y_\alpha + y_{-\alpha}) + (2n - 1) \cdot y_\gamma \end{aligned} \quad (1)$$

and

$$c(D(G)) = 2n \cdot (x_\alpha + x_{-\alpha} + y_\alpha + y_{-\alpha}) + (2n - 1) \cdot (x_\beta + y_\gamma). \quad (2)$$

Then for the link diagram $(a_{2n}^\alpha, 2b_{2n}^\alpha, 3b_{2n-1}^\gamma)$, we have

$$w(D(G)) = (-1) \cdot 2n \cdot 1 + 2n \cdot 2 + (2n - 1) \cdot 3 = 8n - 3$$

and

$$c(D(G)) = 2n \cdot (1 + 2) + (2n - 1) \cdot 3 = 12n - 3.$$

Hence we obtain

$$T(D(G)) = |w(D(G))| = 8n - 3 > \frac{12n - 3}{3} = 4n - 1.$$

By using theorem 3.3, the diagram $(a_{2n}^\alpha, 2b_{2n}^\alpha, 3b_{2n-1}^\gamma)$ is chiral. Similarly, the crossing number and twist number of the remaining OT-link diagrams are all calculated by using the above formulas, as listed in the table 1. Also by using theorem 3.3, they are all chiral. ■

3.3 HOMFLY polynomial of OT-link diagrams

Let f_z^m denote the lowest-degree term of z in the multi-variable polynomial f taken over terms with non-zero coefficients. Let $\mu(D)$ denote the component number for any link diagram D . Hereafter, for the sake of convenience, when we talk about HOMFLY polynomial, it is safe for us to use the link diagram D as a link. Our result begins with the following definition.

Definition 3.5. [22] *The HOMFLY polynomial $H(L) = H(L; v, z) \in \mathbb{Z}[v, z]$ for an oriented link L is defined by the following relationships:*

- (1) $H(L; v, z)$ is invariant under ambient isotopy of L .
- (2) If L is a trivial knot, then $H(L; v, z) = 1$.
- (3) Suppose that three link diagrams L_+ , L_- and L_0 are different only on a local region, as shown in Fig. 5, then $v^{-1}H(L_+; v, z) - vH(L_-; v, z) = zH(L_0; v, z)$.

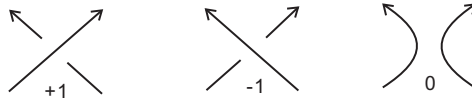


Figure 5. Three link diagrams L_+ , L_- and L_0 differ locally at the site of a single crossing.

The HOMFLY polynomial has the following properties:

- (1) If L is the disjoint union of L_1 and L_2 , denoted by $L_1 \cup L_2$, then

$$H(L_1 \cup L_2) = \left(\frac{v^{-1} - v}{z} \right) H(L_1)H(L_2).$$

- (2) If L^* is the mirror image of L , then

$$H(L^*; v, z) = H(L; -v^{-1}, z).$$

According to this definition, to obtain the HOMFLY polynomial $H(D)$, we need to repeatedly apply the skein relations to the crossings of D until each new resulting link

D_i are all trivial for $i = 1, 2, \dots, s$ ($s \in \mathbb{Z}^+$). In this process, we can assume that no crossing is switched or smoothed more than once [22, 50], and the polynomial produced by switching or smoothing the crossings of D to obtain the trivial link D_i is denoted by $P_i(v, z) \in \mathbb{Z}[v, z]$. Then we have

$$H(D; v, z) = \sum_{i=1}^s P_i(v, z)H(D_i).$$

Also, according to the definition and properties of HOMFLY polynomial, we have

$$P_i(v, z)H(D_i) = h_i(v)z^{m_i} \tag{3}$$

for $h_i(v) \in \mathbb{Z}[v]$ and $m_i \in \mathbb{Z}$. Hence we have

$$H(D; v, z) = \sum_{i=1}^s h_i(v)z^{m_i}.$$

Let m_0 be the lowest degree of z for $H(D)$. Then there exist some trivial links $D_{i'}$ for $1 \leq i' \leq s' \leq s$ ($i', s' \in \mathbb{Z}$) such that

$$\min_z H(D; v, z) = \sum_{i=1}^s P_{i'}(v, z)H(D_{i'}) = \left[\sum_{i=1}^s h_{i'}(v) \right] z^{m_0}. \tag{4}$$

Thus, to obtain the lowest-degree term of z for $H(D)$, we only need to find each diagram $D_{i'}$, which is given in the following lemma.

Lemma 3.6. *Each trivial link $D_{i'}$ in the equation (4) can be obtained from D by only switching some crossings c_1, c_2, \dots, c_t ($t \in \mathbb{N}$) or by first smoothing some of these crossings such that each crossing is exactly on a component of D and then switching some of the remaining crossings of G .*

Proof: Clearly, there exist some crossings c_1, c_2, \dots, c_t such that switching these crossings enable D to become a trivial link diagram D_1 ($t \in \mathbb{N}$). These operations of switching will result in a polynomial

$$P_1(v, z) \in \mathbb{Z}[v, z].$$

Without loss of generality, we assume $s(c_1) = +1$. According to the definition (3) of HOMFLY polynomial, switching the crossing c_1 will produce a term v^2 , but the component number $\mu(D)$ is unchanged. Hence for the diagram D_1 , the related polynomial $P_1(v, z)$ only has the variable v , that is $P_1(v, z) = P_1(v) \in \mathbb{Z}[v]$.

On the other hand, smoothing the crossing c_1 will produce a term vz , and the resulting link diagram is denoted by D' . Meanwhile the component number $\mu(D)$ is changed. Let D_2 be a trivial link diagram obtained from the diagram D' by only switching some crossings, and the related polynomial is denoted by $P''(v) \in \mathbb{Z}[v]$. On the other hand, according to the formula (3), there exists the polynomial $P_2(v, z)H(D_2)$ corresponding to D_2 . Then we have

$$P_2(v, z)H(D_2) = vz \cdot P''(v) \cdot H(D_2).$$

In the following, there will be two cases depending on $\mu(D)$. In one case when $\mu(D') = \mu(D) + 1$, we obtain

$$H(D_2) = (v^{-1} - v)z^{-1}H(D_1).$$

Then

$$\begin{aligned} P_2(v, z)H(D_2) &= vz \cdot P''(v) \cdot H(D_2) \\ &= vz \cdot P''(v) \cdot (v^{-1} - v)z^{-1}H(D_1) \\ &= (1 - v^2)P''(v)H(D_1). \end{aligned}$$

Hence $P_2(v, z)H(D_2)$ and $P_1(v)H(D_1)$ have the same degree over the variable z .

In other case when $\mu(D') = \mu(D) - 1$, we obtain

$$H(D_2) = (v^{-1} - v)^{-1}zH(D_1).$$

Then

$$\begin{aligned} P_2(v, z)H(D_2) &= vz \cdot P''(v) \cdot H(D_2) \\ &= vz \cdot P''(v) \cdot (v^{-1} - v)^{-1}zH(D_1) \\ &= \frac{vz^2}{v^{-1} - v}P''(v)H(D_1). \end{aligned}$$

Hence the degree of z is two higher in $P_2(v, z)H(D_2)$ than in $P_1(v)H(D_1)$.

Then $P_1(v, z)H(D_1)$ is a lowest-degree term of z for $H(D_1)$. Therefore, if the crossing c_1 is on the same component of D , smoothing it will enable $\mu(D)$ to increase by one. As shown above, the corresponding polynomial $P_2(v, z)H(D_2)$ is also a lowest-degree term of z for $H(D)$.

In general, smooth any r crossings among the crossings c_1, c_2, \dots, c_t such that each crossing is exactly on a component of D , and then switch some of the remaining crossings

of D to obtain a trivial link diagram D_3 . As shown above, the corresponding polynomial $P_3(v, z)H(D_3)$ is exactly a lowest-degree term of z for $H(D)$. The lemma 7 holds. ■

On the other hand, using the definition of HOMFLY polynomial, we also obtain the following lemmas.

Lemma 3.7. *Let $D_{a_{2n}^\alpha}$ be a link diagram with an oriented twist tangle a_{2n}^α ($n \in \mathbb{Z}^+$), and $D_{a_{2k}^\alpha}$ be the same as $D_{a_{2n}^\alpha}$ except the tangle a_{2k}^α for $k = 1, 2, \dots, n - 1$. Let $D_{a_0^\alpha}$ and $D_{a_\infty^\alpha}$ be two link diagrams obtained from the link diagram $D_{a_2^\alpha}$ by switching and smoothing a crossing of a_2^α respectively. Then*

$$H(D_{a_{2n}^\alpha}) = v^{-2n}H(D_{a_0^\alpha}) - v^{-1}z\frac{v^{-2n} - 1}{v^{-2} - 1}H(D_{a_\infty^\alpha}). \quad (5)$$

Proof: We proceed by induction on the crossing number $2n$ of a_{2n}^α . Obviously, this lemma holds for $n = 1$. Now we suppose that $n \geq 2$. Applying the skein relation of HOMFLY polynomial to a crossing of a_{2n}^α , we obtain

$$H(D_{a_{2n}^\alpha}) = v^{-2}H(D_{a_{2n-2}^\alpha}) - v^{-1}zH(D_{a_\infty^\alpha}).$$

By applying our induction hypothesis to the link diagram $D_{a_{2n-2}^\alpha}$, we have

$$\begin{aligned} H(D_{a_{2n}^\alpha}) &= v^{-2} \left[v^{-(2n-2)}H(D_{a_0^\alpha}) - v^{-1}z\frac{v^{-(2n-2)} - 1}{v^{-2} - 1}H(D_{a_\infty^\alpha}) \right] \\ &\quad - v^{-1}zH(D_{a_\infty^\alpha}) = v^{-2n}H(D_{a_0^\alpha}) - v^{-1}z\frac{v^{-2n} - 1}{v^{-2} - 1}H(D_{a_\infty^\alpha}). \end{aligned}$$

■

Similarly, we obtain the following lemma 2.

Lemma 3.8. *Let $D_{b_{2n}^\alpha}$ be a link diagram with an oriented twist tangle b_{2n}^α ($n \in \mathbb{Z}^+$), and $D_{b_{2k}^\alpha}$ be the same as $D_{b_{2n}^\alpha}$ except the tangle b_{2k}^α for $k = 1, 2, \dots, n - 1$. Let $D_{b_0^\alpha}$ and $D_{b_\infty^\alpha}$ be two link diagrams obtained from $D_{b_2^\alpha}$ by switching and smoothing a crossing of b_2^α respectively. Then*

$$H(D_{b_{2n}^\alpha}) = v^{2n}H(D_{b_0^\alpha}) + vz\frac{v^{2n} - 1}{v^2 - 1}H(D_{b_\infty^\alpha}). \quad (6)$$

Lemma 3.9. *Let $D_{b_{2n-1}^\gamma}$ be a link diagram with an oriented twist tangle b_{2n-1}^γ ($n \in \mathbb{Z}^+$), and $D_{b_{2k-1}^\gamma}$ be the same as $D_{b_{2n-1}^\gamma}$ except the tangle b_{2k-1}^γ for $k = 1, 2, \dots, n - 1$. Let $D_{b_{-1}^\gamma}$ and $D_{b_\infty^\gamma}$ be two link diagrams obtained from $D_{b_1^\gamma}$ by switching and smoothing a crossing*

of b_1^γ respectively. Then

$$H(D_{b_{2n-1}^\gamma}) = v^{2n-2}H(D_{b_1^\gamma}) + vz\frac{v^{2n-2}-1}{v^2-1}H(D_{b_\infty^\gamma}) \quad (7)$$

$$\text{and} \quad H(D_{b_{2n-1}^\gamma}) = v^{2n}H(D_{b_{-1}^\gamma}) + vz\frac{v^{2n}-1}{v^2-1}H(D_{b_\infty^\gamma}). \quad (8)$$

Proof: We proceed by induction on the crossing number $2n-1$ of b_{2n-1}^γ . Obviously, the lemma holds for $n=1$. Now we suppose that $n \geq 2$. Applying the definition (3) of HOMFLY polynomial to a crossing of b_{2n-1}^γ , we obtain

$$H(D_{b_{2n-1}^\gamma}) = v^2H(D_{b_{2n-2}^\gamma}) + v^{-1}zH(D_{b_\infty^\gamma}).$$

By applying our induction hypothesis to the link diagram $D_{b_{2n-2}^\gamma}$, we have

$$\begin{aligned} H(D_{b_{2n}^\gamma}) &= v^2 \left[v^{2n-4}H(D_{b_1^\gamma}) + vz\frac{v^{2n-4}-1}{v^2-1}H(D_{b_\infty^\gamma}) \right] \\ &+ vzH(D_{b_\infty^\gamma}) = v^{2n-2}H(D_{b_1^\gamma}) + (vz\frac{v^{2n-2}-v^2}{v^2-1} + vz)H(D_{b_\infty^\gamma}) \\ &= v^{2n-2}H(D_{b_1^\gamma}) + vz\frac{v^{2n-2}-1}{v^2-1}H(D_{b_\infty^\gamma}). \end{aligned}$$

Also,

$$H(D_{b_1^\gamma}) = v^2H(D_{b_{-1}^\gamma}) + vzH(D_{b_\infty^\gamma}).$$

Hence we have

$$\begin{aligned} H(D_{b_{2n}^\gamma}) &= v^{2n-2} \left[v^2H(D_{b_{-1}^\gamma}) + vzH(D_{b_\infty^\gamma}) \right] + vz\frac{v^{2n-2}-1}{v^2-1}H(D_{b_\infty^\gamma}) \\ &= v^{2n}H(D_{b_{-1}^\gamma}) + vz\frac{v^{2n}-1}{v^2-1}H(D_{b_\infty^\gamma}). \end{aligned}$$

■

By using the above lemmas and setting $\delta = \frac{v^{-1}-v}{z}$, we obtain the following theorem.

Theorem 3.10.

- (1) $H_z^m(D(a_{2n}^\alpha, 3b_{2n}^\alpha, a_{2n}^\alpha, b_{2n}^\alpha)) = v^{8n} \delta.$
- (2) $H_z^m(D(2a_{2n}^\alpha, b_{2n}^\alpha, 3b_{2n-1}^\gamma)) = v^{2n-2} \delta.$
- (3) $H_z^m(D(2a_{2n}^\alpha, 4b_{2n}^\alpha)) = (v^{8n} + v^{2n} - v^{4n}) \delta.$
- (4) $H_z^m(D(3a_{2n}^\alpha, 3b_{2n-1}^\gamma)) = v^{-6n} - 3v^{-2n-2} + 3v^{-2}.$
- (5) $H_z^m(D(a_{2n}^\alpha, 3b_{2n-1}^\gamma, a_{2n}^{-\alpha}, b_{2n-1}^\gamma)) = (2v^{6n-4} - v^{4n-4}) \delta.$
- (6) $H_z^m(D(3a_{2n}^\alpha, 3b_{2n}^\alpha)) = v^{6n} - 3v^{2n} - 3v^{-2n} + 5 + v^{-6n}.$
- (7) $H_z^m(D(b_{2n}^\alpha, 3b_{2n-1}^\gamma, b_{2n}^{-\alpha}, b_{2n-1}^\gamma)) = (2v^{10n-4} - v^{12n-4}) \delta.$
- (8) $H_z^m(D(3b_{2n}^\alpha, 3b_{2n-1}^\gamma)) = (-v^{12n-2} - v^{12n-4} + 3v^{10n-2}) \delta.$
- (9) $H_z^m(D(a_{2n}^\alpha, 3b_{2n}^\alpha, 2a_{2n}^\alpha)) = v^{6n} - 2v^{2n} - 2v^{-2n} + 3 + v^{-6n}.$
- (10) $H_z^m(D(a_{2n}^\alpha, 2b_{2n}^\alpha, 3b_{2n-1}^\gamma)) = -v^{10n-4} - v^{10n-2} + 3v^{8n-2} + 2v^{4n-2} - 2v^{6n-2}.$

Proof:(1) There is only one lowest-degree term of z for $H(D(a_{2n}^\alpha, 3b_{2n}^\alpha, a_{2n}^\alpha, b_{2n}^\alpha))$. First, the link diagram $D = D(a_{2n}^\alpha, 3b_{2n}^\alpha, a_{2n}^\alpha, b_{2n}^\alpha)$ is changed into a trivial link diagram D_1 of two components by switching n crossings of each twist tangle b_{2n}^α (Fig. 6(a) and (b)). The resulting polynomial is denoted by $P_1(v, z)$. Since switching n crossings for each twist tangle b_{2n}^α will produce a term v^{2n} according to the lemma 3.8, we have

$$P_1(v, z) = (v^{2n})^4 = v^{8n}.$$

Also, using the property (2) of HOMFLY polynomial, we have

$$P_1(v, z)H(D_1) = v^{8n} \delta.$$

In addition, each twist diagram b_{2n}^α for the link diagram D is composed of two different components. By using the lemma 7, smoothing any crossing of b_{2n}^α -twist don't result in a lowest-degree term of z for $H(D)$. Thus we have

$$H_z^m(D) = v^{8n} \delta.$$

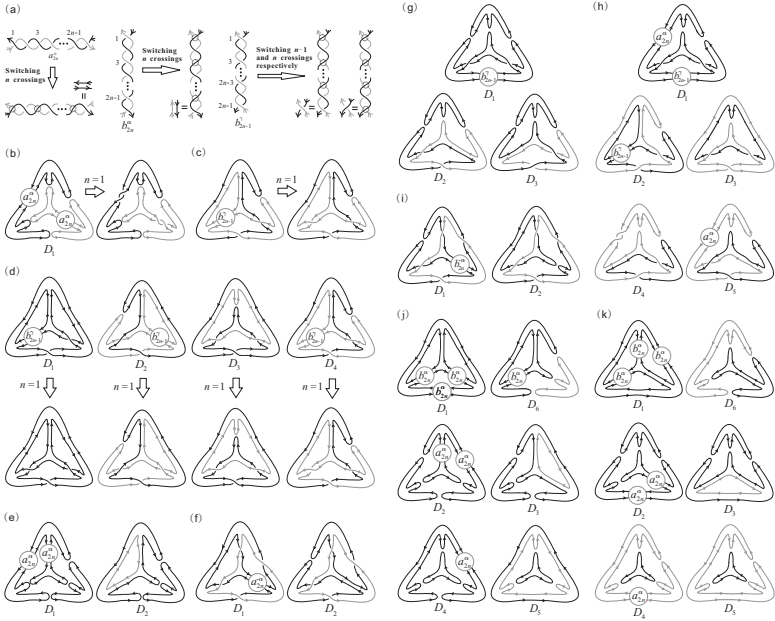


Figure 6. (a) For each twist tangle, each crossing switched is bounded by a circle. (b-k) Each disk labeled with a_{2n}^α , b_{2n}^α , b_{2n-1}^α or b_{2n-1}^γ represent the corresponding oriented twist tangle in each diagram D_i for $1 \leq i \leq 6$. In particular, D_i in the case of $n = 1$ is given in (b-d).

(2) There is only one lowest-degree term of z of $H(D(2a_{2n}^\alpha, b_{2n}^\alpha, 3b_{2n-1}^\gamma))$. First, the link diagram $D = D(2a_{2n}^\alpha, b_{2n}^\alpha, 3b_{2n-1}^\gamma)$ is changed into a trivial link diagram D_1 of two components by switching the crossings of all oriented twist tangles except a b_{2n-1}^γ (Fig. 6(a) and (c)). In this process, we switch n crossings of each a_{2n}^α , n crossings of a b_{2n}^α , n crossings of one b_{2n-1}^γ and switching $n - 1$ crossings of the other b_{2n-1}^γ . By using the lemmas 3.7-3.9, then the resulting polynomial $P_1(v, z)$ is given as

$$P_1(v, z) = (v^{-2n})^2 \cdot v^{2n} \cdot v^{2n} \cdot v^{2n-2} = v^{2n-2}.$$

Hence we obtain

$$P_1(v, z)H(D_1) = v^{2n-2}\delta.$$

In addition, for the link diagram D , each twist tangle except an unused b_{2n-1}^γ is composed of two different components. For each such tangle, smoothing its any crossing

don't result in a lowest-degree term of z for $H(D)$ by using the lemma 3.6. Thus we have

$$H_z^m(D) = v^{2n-2}\delta.$$

(3) There are two trivial link diagrams, which both result in the lowest-degree terms of z for $H(D(2a_{2n}^\alpha, 4b_{2n}^\alpha))$. First, the link diagram $D = D(2a_{2n}^\alpha, 4b_{2n}^\alpha)$ will be changed into a trivial link diagram D_1 of two components by switching n crossings of each twist tangle b_{2n}^α (Fig. 6(a) and (e)). The resulting polynomial is $P_1(v, z) = (v^{2n})^4$ by using the lemma 3.8. Then we obtain

$$H(D_1)P_1(v, z) = \delta \cdot (v^{2n})^4 = v^{8n}\delta.$$

On the other hand, there is only one twist tangle b_{2n}^α on the same component of D . Smoothing n crossings of this twist tangle b_{2n}^α , the link diagram D is changed into a link diagram D'_2 of three components, which will produce a term $vz\frac{v^{2n}-1}{v^2-1}$ by using the lemma 3.8. The diagram D'_2 is further changed into a trivial link D_2 by switching n crossings of the remaining each twist tangle (Fig. 6(e)), which will produce the polynomial $(v^{2n})^3 \cdot (v^{-2n})^2$ by using the lemmas 3.7 and 3.8. Then for the polynomial $P_2(v, z)$ related to D_2 , we have

$$P_2 = vz\frac{v^{2n}-1}{v^2-1} \cdot (v^{2n})^3 \cdot (v^{-2n})^2 = vz\frac{v^{4n}-v^{2n}}{v^2-1}.$$

Also, we have

$$H(D_2) = \delta^2.$$

Then we obtain

$$P_2(v, z)H(D_2) = vz\frac{v^{4n}-v^{2n}}{v^2-1}\delta^2 = (v^{2n}-v^{4n})\delta.$$

By using the lemma 3.7, the lowest-degree term of z for $H(D)$ only contains the above two cases, and then we have

$$H_z^m(D) = H(D_1)P_1(v, z) + H(D_2)P_2(v, z) = v^{8n}\delta + (v^{2n}-v^{4n})\delta = (v^{8n} + v^{2n} - v^{4n})\delta.$$

(4) There are four trivial link diagrams, which all together result in the lowest-degree term of z for $H(D(3a_{2n}^\alpha, 3b_{2n-1}^\gamma))$. A trivial knot D_1 is obtained from the diagram $D = D(3a_{2n}^\alpha, 3b_{2n-1}^\gamma)$ by switching n crossings of each twist tangle a_{2n}^α (Fig. 6(a) and (d)). These operations produce the polynomial $P_1(v, z) = (v^{-2n})^3$ by using the lemma 3.7. Hence we have

$$P_1(v, z) \cdot H(D_1) = (v^2)^{3n} \cdot 1 = v^{-6n}.$$

On the other hand, due to each twist tangle a_{2n}^α on the same component, three link diagrams D'_2, D'_3 and D'_4 are obtained from the diagram $D(3a_{2n}^\alpha, 3b_{2n-1}^\gamma)$ by smoothing n crossings of each twist tangle a_{2n}^α respectively. And then each link D'_i is further changed into a trivial link D_i for $2 \leq i \leq 4$ by switching the crossings of the remaining twist tangles except a twist tangle a_{2n-1}^β consisting of two components (Fig. 6(d)). In this process, we switch n crossings of the remaining each a_{2n}^α , $n-1$ crossings of one b_{2n}^γ and n crossings of the other b_{2n}^γ (Fig. 6(a)). Also, switching or smoothing n crossings of a twist tangle a_{2n}^α will result in a term v^{-2n} or $-v^{-1}z\frac{v^{-2n}-1}{v^{-2}-1}$ by using the lemma 3.7, and switching n or $n-1$ crossings of a twist tangle b_{2n-1}^γ will result in a term v^{2n} or $v^{2(n-1)}$ by using the lemma 3. Then the resulting polynomial $P_i(v, z)$ is given as

$$P_i(v, z) = -v^{-1}z\frac{v^{-2n}-1}{v^{-2}-1} \cdot (v^{-2n})^2 \cdot v^{2n} \cdot v^{2n-2} = -v^{-3}z\frac{v^{-2n}-1}{v^{-2}-1}.$$

Also, each trivial link diagram D_i consists of two components, then

$$H(D_i) = \delta.$$

Hence we have

$$\prod_{i=2}^4 P_i(v, z)H(D_i) = \prod_{i=2}^4 \left[\left(-v^{-3}z\frac{v^{-2n}-1}{v^{-2}-1} \right) \cdot \delta \right] = 3(-v^{-2n-2} + v^{-2}).$$

According to the lemma 3.6, the lowest-degree term of z for $H(3a_{2n}^\alpha, 3b_{2n-1}^\gamma)$ only contains the above four cases, hence we have

$$H_z^m(D) = \prod_{i=1}^4 P_i(v, z)H(D_i) = v^{-6n} - 3v^{-2n-2} + 3v^{-2}.$$

(5) There are two trivial link diagrams, which both result in the lowest-degree terms of z for $H(D(a_{2n}^\alpha, 3b_{2n-1}^\gamma, a_{2n}^{-\alpha}, b_{2n-1}^\gamma))$. First, this link $D = D(a_{2n}^\alpha, 3b_{2n-1}^\gamma, a_{2n}^{-\alpha}, b_{2n-1}^\gamma)$ is changed into a trivial link D_1 of two components by switching some crossings (Fig. 6(f)). In this process, switch n crossings of each for two b_{2n-1}^γ and a a_{2n}^α , and $n-1$ crossings of each of the remaining two b_{2n-1}^γ (Fig. 6(a)). The resulting polynomial $P_1(v, z)$ is that

$$P_1(v, z) = v^{-2n} \cdot (v^{2n})^2 \cdot (v^{2n-2})^2.$$

by using the lemmas 3.7 and 3.9. Hence we have

$$P_1(v, z)H(D_1) = v^{6n-4} \cdot \delta.$$

On the other hand, for the above five twist tangles we used, there is only one a_{2n}^α on the same component of D . Switching n crossings of this twist tangle a_{2n}^α , we can obtain the link diagram D'_2 from D , which will produce a term $-v^{-1}z\frac{v^{-2n}-1}{v^{-2}-1}$ by using lemma 3.7. Then D'_2 is further changed into a trivial link D_2 by switching the crossings of the remaining twist tangles. In this process, switch n crossings of each for two b_{2n}^γ and a a_{2n}^α , and $n-1$ crossings of each for the remaining two b_{2n}^γ . Hence for the polynomial $P_2(v, z)$ corresponding to D_2 , we have

$$P_2(v, z) = \left(-v^{-1}z\frac{v^{-2n}-1}{v^{-2}-1} \right) \cdot v^{6n-4}.$$

Hence we obtain

$$P_2(v, z)H(D_2) = \frac{v^{6n-4} - v^{4n-4}}{v^{-1} - v} z \cdot \delta^2 = (v^{6n-4} - v^{4n-4})\delta.$$

Then

$$\begin{aligned} H_z^m(D) &= P_1(v, z)H(D_2) + P_2(v, z)H(D_2) \\ &= v^{6n-4} \cdot \delta + (v^{6n-4} - v^{4n-4})\delta \\ &= (2v^{6n-4} - v^{4n-4})\delta. \end{aligned}$$

(6) There are six trivial link diagrams, which all together result in the lowest-degree term of z for $H(D(3a_{2n}^\alpha, 3b_{2n}^\alpha))$. A trivial knot D_1 is obtained from the diagram $D = D(3a_{2n}^\alpha, 3b_{2n}^\alpha)$ by switching n crossings of each twist tangle a_{2n}^α (Fig. 6(a) and Fig. 7(d)). The resulting polynomial $P_1(v, z)$ is given as

$$P_1(v, z) = (v^{-2n})^3$$

by using the lemma 3.7. Then we have

$$P_1(v, z) \cdot H(D_1) = (v^2)^{3n} \cdot 1 = v^{-6n}.$$

On the other hand, we note that three a_{2n}^α are all on the same component of D . First, we smooth n crossings of a a_{2n}^α to obtain the link diagram D'_2 from D . Then D'_2 is further changed into a trivial link diagram D_2 by switching n crossings of each b_{2n}^α (Fig. 7(d)). Then the resulting polynomial $P_2(v, z)$ is given as

$$P_2(v, z)H = \left(-v^{-1}z\frac{v^{-2n}-1}{v^{-2}-1} \right) \cdot (v^{2n})^3$$

by using the lemmas 3.7 and 3.8. Hence we obtain

$$P_2(v, z)H(D_2) = \left(-v^{-1}z \frac{v^{-2n} - 1}{v^{-2} - 1}\right) v^{6n} \cdot \delta = v^{6n} - v^{4n}.$$

Also, there is only one b_{2n}^α on the same component of D'_2 . Then D'_2 is also changed into a trivial link D_3 by smoothing n crossings of the b_{2n}^α and switching n crossings of the remaining each twist tangle (Fig. 7(d)). Then the resulting polynomial $P_3(v, z)$ is given as

$$P_3(v, z) = \left(-v^{-1}z \frac{v^{-2n} - 1}{v^{-2} - 1}\right) \cdot (v^{-2n})^2 \cdot (v^{2n})^2 \cdot v z \frac{v^{2n} - 1}{v^2 - 1}.$$

Hence we obtain

$$P_3(v, z)H(D_3) = \left(-v^{-1}z \frac{v^{-2n} - 1}{v^{-2} - 1}\right) v z \frac{v^{2n} - 1}{v^2 - 1} \cdot \delta = 2 - v^{-2n} - v^{2n}.$$

Second, we smooth n crossings of another a_{2n}^α and keep switching n crossings of a a_{2n}^α to obtain the link diagram D'_4 from D . Then D'_4 is further changed into a trivial link D_4 by switching n crossings of each b_{2n}^α (Fig. 7(d)). Then the resulting polynomial $P_4(v, z)$ is given as

$$P_4(v, z) = \left(-v^{-1}z \frac{v^{-2n} - 1}{v^{-2} - 1}\right) \cdot v^{-2n} \cdot (v^{2n})^3.$$

Hence we obtain

$$P_4(v, z)H(D_4) = \left(-v^{-1}z \frac{v^{-2n} - 1}{v^{-2} - 1}\right) v^{4n} \cdot \delta = v^{4n} - v^{2n}.$$

Also, there is a b_{2n}^α on the same component of the link diagram D'_4 . Then D'_4 is further changed into a trivial link D_5 by smoothing n crossings of the b_{2n}^α and switching n crossings of the remaining each twist tangle (Fig. 7(d)). Then the resulting polynomial $P_5(v, z)$ is given as

$$P_5(v, z) = \left(-v^{-1}z \frac{v^{-2n} - 1}{v^{-2} - 1}\right) \cdot (v^{-2n})^2 \cdot (v^{2n})^2 \cdot v z \frac{v^{2n} - 1}{v^2 - 1}.$$

Hence we obtain

$$P_5(v, z)H(D_5) = \left(-v^{-1}z \frac{v^{-2n} - 1}{v^{-2} - 1}\right) v z \frac{v^{2n} - 1}{v^2 - 1} \cdot \delta = 2 - v^{-2n} - v^{2n}.$$

At last, we smooth n crossings of the third twist tangle a_{2n}^α and keep switching n crossings of each for the remaining two a_{2n}^α to obtain D'_6 from D . Then D'_6 is further

changed into a trivial link D_6 by switching n crossings of each for two b_{2n}^α (Fig. 7(d)).

Then the resulting polynomial $P_6(v, z)$ is given as

$$P_6(v, z) = \left(-v^{-1}z \frac{v^{-2n} - 1}{v^{-2} - 1} \right) \cdot (v^{-2n})^2 \cdot (v^{2n})^2.$$

Hence we obtain

$$P_6(v, z)H(D_6) = \left(-v^{-1}z \frac{v^{-2n} - 1}{v^{-2} - 1} \right) \cdot \delta = 1 - v^{-2n}.$$

According to the lemma 3.6, the lowest-degree term of z for $H(D(3a_{2n}^\alpha, 3b_{2n}^\alpha))$ only contains the above six cases, hence we have

$$\begin{aligned} H_z^m(D) &= \prod_{i=1}^6 P_i(v, z)H(D_i) \\ &= v^{-6n} + (v^{6n} - v^{4n}) + (2 - v^{-2n} - v^{2n}) + (v^{4n} - v^{2n}) \\ &\quad + (2 - v^{-2n} - v^{2n}) + (1 - v^{-2n}) \\ &= v^{6n} - 3v^{2n} + 5 - 3v^{-2n} + v^{-6n}. \end{aligned}$$

(7) There are two trivial link diagrams, which both result in the lowest-degree term of z for $H(D(b_{2n}^\alpha, 3b_{2n-1}^\gamma, b_{2n}^{-\alpha}, b_{2n-1}^\gamma))$. A trivial link diagram D_1 of two component is obtained from the diagram $D = D(b_{2n}^\alpha, 3b_{2n-1}^\gamma, b_{2n}^{-\alpha}, b_{2n-1}^\gamma)$ by switching some crossings. In this process, we switch n crossings of each for a b_{2n}^α and two b_γ^α , and switch $n - 1$ crossings of each for the other two b_γ^α (Fig. 6(a) and Fig. 7(c)). Then the resulting polynomial $P_1(v, z)$ is given as

$$P_1(v, z) = (v^{2n})^3 (v^{2n-2})^2.$$

by using the lemmas 3.8 and 3.9. Hence we obtain

$$P_1(v, z)H(D_1) = v^{10n-4}\delta.$$

On the other hand, there is only one b_{2n}^α is on the same component of D . We smooth n crossings of b_{2n}^α and switch n crossings of each for a $b_{2n}^{-\alpha}$ and two b_γ^α , and then switch $n - 1$ crossings of each for the remaining two b_γ^α to obtain a trivial link diagrams D_2 of three components (Fig. 7(c)). Then the resulting polynomial $P_2(v, z)$ is given as

$$P_2(v, z) = v z \frac{v^{2n} - 1}{v^2 - 1} \cdot (v^{2n})^3 \cdot (v^{2n-2})^2.$$

Hence we obtain

$$P_2(v, z)H(D_2) = vz \frac{v^{2n} - 1}{v^2 - 1} v^{10n-4} \cdot \delta^2 = v^{10n-4}(1 - v^{2n})\delta.$$

By using the lemma 3.6, hence we have

$$\begin{aligned} H_z^m(D) &= P_1(v, z)H(D_1) + P_2(v, z)H(D_2) \\ &= v^{10n-4}\delta + v^{10n-4}(1 - v^{2n})\delta \\ &= (2v^{10n-4} - v^{12n-4})\delta. \end{aligned}$$

(8) There are three trivial link diagrams, which all together result in the lowest-degree term of z for $H(D(3b_{2n}^\alpha, 3b_{2n-1}^\gamma))$. The diagram $D = D(3b_{2n}^\alpha, 3b_{2n-1}^\gamma)$ is changed into a trivial link diagram D_1 by switching some crossings. In this process, we switch n crossings of each for three b_{2n}^α and a b_{2n-1}^γ , and switch $n - 1$ crossings of another b_{2n-1}^γ (Fig. 6(a) and Fig. 7(a)). Then the resulting polynomial $P_1(v, z)$ is given as

$$P_1(v, z) = (v^{2n})^4 \cdot v^{2n-2}.$$

by using the lemmas 3.8 and 3.9. Hence we have

$$P_1(v, z)H(D_1) = v^{10n-2}\delta.$$

Note that two b_{2n}^α in the above process are both on the same component of D . First, we smooth n crossings of one b_{2n-1}^γ , and switch n crossings of each for three b_{2n}^α and another b_{2n-1}^γ , and then switch $n - 1$ crossings of the remaining b_{2n-1}^γ to obtain the trivial link diagram D_2 of three components from D (Fig. 6(a) and Fig. 7(a)). Then the resulting polynomial $P_2(v, z)$ is given as

$$P_2(v, z) = vz \frac{v^{2n} - 1}{v^2 - 1} \cdot (v^{2n})^4 \cdot v^{2n-2}.$$

Hence we obtain

$$P_2(v, z)H(D_2) = vz \frac{v^{2n} - 1}{v^2 - 1} v^{10n-2} \cdot \delta^2 = v^{10n-2}(1 - v^{2n})\delta.$$

On the other hand, we smooth $n - 1$ crossings of the other b_{2n-1}^γ and keep switching n crossings of each for three b_{2n}^α and a b_{2n-1}^γ , and then switch $n - 1$ crossings of the remaining b_{2n-1}^γ to obtain the trivial link diagram D_3 of three components. Then the resulting polynomial is given as

$$P_3(v, z) = vz \frac{v^{2n-2} - 1}{v^2 - 1} \cdot (v^{2n})^4 \cdot v^{2n-2}.$$

Hence we obtain

$$P_3(v, z)H(D_2) = v^{10n-2}(1 - v^{2n-2})\delta.$$

According to the lemma 3.6, the lowest-degree term of z for $H(D(3b_{2n}^\alpha, 3b_{2n-1}^\gamma))$ only contains the above three cases, hence we have

$$\begin{aligned} H_z^m(D) &= \prod_{i=1}^3 P_i(v, z)H(D_i) \\ &= v^{10n-2}\delta + v^{10n-2}(1 - v^{2n})\delta + v^{10n-2}(1 - v^{2n-2})\delta \\ &= (3v^{10n-2} - v^{12n-2} - v^{12n-4})\delta. \end{aligned}$$

(9) There are six trivial link diagrams, which all together result in the lowest-degree term of z for $H(D(a_{2n}^\alpha, 3b_{2n}^\alpha, 2a_{2n}^\alpha))$. A trivial knot D_1 is obtained from the diagram $D = D(3a_{2n}^\alpha, 3b_{2n}^\alpha)$ by switching n crossings of each twist tangle a_{2n}^α (Fig. 6(a) and Fig. 7(e)). Then the resulting polynomial $P_1(v, z)$ is given as

$$P_1(v, z) = (v^{-2n})^3$$

by using the lemma 3.7. Hence we have

$$P_1(v, z) \cdot H(D_1) = v^{-6n}.$$

On the other hand, we note that three a_{2n}^α are all on the same component of D . First, we smooth n crossings of a a_{2n}^α to obtain the link diagram D'_2 . Then D'_2 is further changed into a trivial link diagram D_2 by switching n crossings of each b_{2n}^α (Fig. 6(a) and Fig. 7(e)). The resulting polynomial $P_2(v, z)$ is given as

$$P_2(v, z) = \left(-v^{-1}z \frac{v^{-2n} - 1}{v^{-2} - 1}\right) \cdot (v^{2n})^3$$

by using the lemmas 3.7 and 3.8. Hence we obtain

$$P_2(v, z)H(D_2) = \left(-v^{-1}z \frac{v^{-2n} - 1}{v^{-2} - 1}\right) v^{6n} \cdot \delta = v^{6n} - v^{4n}.$$

Also, there is only one b_{2n}^α on the same component of D'_2 . Then D'_2 is further changed into a trivial link diagram D_3 by smoothing n crossings of the b_{2n}^α and switching n crossings of the remaining each twist tangle. The resulting polynomial $P_3(v, z)$ is given as

$$P_3(v, z) = \left(-v^{-1}z \frac{v^{-2n} - 1}{v^{-2} - 1}\right) \cdot (v^{-2n})^2 \cdot (v^{2n})^2 \cdot v z \frac{v^{-2n} - 1}{v^{-2} - 1}.$$

Hence we obtain

$$P_3(v, z)H(D_3) = \left(-v^{-1}z \frac{v^{-2n} - 1}{v^{-2} - 1}\right) \cdot vz \frac{v^{-2n} - 1}{v^2 - 1} \cdot \delta^2 = 2 - v^{-2n} - v^{2n}.$$

Second, we smooth n crossings of another a_{2n}^α and keep switching n crossings of a a_{2n}^α to obtain D'_4 . Then D'_4 is further changed into a trivial link D_4 by switching n crossings of each b_{2n}^α (Fig. 7(e)). Then the resulting polynomial $P_4(v, z)$ is given as

$$P_4(v, z) = \left(-v^{-1}z \frac{v^{-2n} - 1}{v^{-2} - 1}\right) \cdot v^{-2n} \cdot (v^{2n})^3.$$

Hence we obtain

$$P_4(v, z)H(D_4) = \left(-v^{-1}z \frac{v^{-2n} - 1}{v^{-2} - 1}\right) v^{4n} \cdot \delta = v^{4n} - v^{2n}.$$

Also, there is only one b_{2n}^α on the same component of D'_4 . Then D'_4 is changed into a trivial link D_5 by smoothing n crossings of the b_{2n}^α and switching n crossings of the remaining each twist tangle (Fig. 7(e)). Then the resulting polynomial $P_5(v, z)$ is given as

$$P_5(v, z) = \left(-v^{-1}z \frac{v^{-2n} - 1}{v^{-2} - 1}\right) \cdot (v^{-2n})^2 \cdot (v^{2n})^2 \cdot vz \frac{v^{-2n} - 1}{v^2 - 1}.$$

Hence we obtain

$$P_5(v, z)H(D_5) = \left(-v^{-1}z \frac{v^{-2n} - 1}{v^{-2} - 1}\right) vz \frac{v^{-2n} - 1}{v^2 - 1} \cdot \delta^2 = 2 - v^{-2n} - v^{2n}.$$

At last, we smooth n crossings of the remaining twist tangle a_{2n}^α and keep switching n crossings of each for the other two a_{2n}^α to obtain D'_6 . Then D'_6 is further changed into a trivial link D_6 by switching n crossings of each b_{2n}^α (Fig. 6(a) and Fig. 7(e)). The resulting polynomial $P_6(v, z)$ is given as

$$P_6(v, z)H(D_6) = \left(-v^{-1}z \frac{v^{-2n} - 1}{v^{-2} - 1}\right) \cdot (v^{-2n})^2 \cdot (v^{2n})^3.$$

Hence we obtain

$$P_6(v, z)H(D_6) = \left(-v^{-1}z \frac{v^{-2n} - 1}{v^{-2} - 1}\right) v^{2n} \cdot \delta = v^{2n} - 1.$$

According to the lemma 3.6, the lowest-degree term of z for $H(D(a_{2n}^\alpha, 3b_{2n}^\alpha, 2a_{2n}^\alpha))$ only contains the above six cases, hence we have

$$\begin{aligned} H_z^m(D) &= \prod_{i=1}^6 P_i(v, z)H(D_i) \\ &= v^{-6n} + (v^{6n} - v^{4n}) + (2 - v^{-2n} - v^{2n}) + (v^{4n} - v^{2n}) \\ &\quad + (2 - v^{-2n} - v^{2n}) + (v^{2n} - 1) \\ &= v^{6n} - 2v^{2n} + 3 - 2v^{-2n} + v^{-6n}. \end{aligned}$$

(10) There are five trivial link diagrams, which all together result in the lowest-degree term of z for $H(D(a_{2n}^\alpha, 2b_{2n}^\alpha, 3b_{2n-1}^\gamma))$. The diagram $D = D(a_{2n}^\alpha, 2b_{2n}^\alpha, 3b_{2n-1}^\gamma)$ is changed into a trivial knot D_1 by switching some crossings. In this process, we switch n crossings of each for two b_{2n}^α and a b_{2n-1}^γ , and switching $n - 1$ crossings of a b_{2n-1}^γ (Fig. 6(a) and Fig. 7(b)). Then the resulting polynomial $P_1(v, z)$ is given as

$$P_1(v, z) = (v^{2n})^3 \cdot v^{2n-2}$$

by using the lemmas 3.8 and 3.9. Then

$$P_1(v, z)H(D_1) = v^{8n-2}.$$

On the other hand, we note that two b_{2n}^α and two b_{2n-1}^γ in the above process are all on the same component of D . First, we smooth n crossings of one b_{2n}^α , and switch n crossings of each for the other b_{2n}^α , a a_{2n}^α and one b_{2n-1}^γ , and switch $n - 1$ crossings of another b_{2n-1}^γ to obtain the trivial link diagram D_2 (Fig. 6(a) and Fig. 7(b)). Then the resulting polynomial $P_2(v, z)$ is given as

$$P_2(v, z) = vz \frac{v^{2n} - 1}{v^2 - 1} \cdot v^{-2n} \cdot (v^{2n})^2 \cdot v^{2n-2}$$

by using the lemmas 3.7-3.9. Hence we obtain

$$P_2(v, z)H(D_2) = vz \frac{v^{2n} - 1}{v^2 - 1} v^{4n-2} \cdot \delta = v^{4n-2} - v^{6n-2}.$$

Second, we smooth n crossings of the other b_{2n}^α and keep switching n crossings of the remaining b_{2n}^α , and then switch n crossings of each for a a_{2n}^α and one b_{2n-1}^γ , and switch $n - 1$ crossings of another b_{2n-1}^γ to obtain the trivial link diagram D_3 of two components from D (Fig. 6(a) and Fig. 7(b)). Then the corresponding polynomial $P_3(v, z)$ is given as

$$P_3(v, z) = vz \frac{v^{2n} - 1}{v^2 - 1} \cdot v^{-2n} \cdot (v^{2n})^2 \cdot v^{2n-2}.$$

Hence we obtain

$$P_3(v, z)H(D_4) = vz \frac{v^{2n} - 1}{v^2 - 1} v^{4n-2} \cdot \delta = v^{4n-2} - v^{6n-2}.$$

Third, we smooth n crossings of one b_{2n-1}^γ and keep switching n crossings of each b_{2n}^α , and then switch n crossings of another b_{2n-1}^γ , and switch $n - 1$ crossings of the remaining

b_{2n-1}^γ to obtain a trivial link D_4 of two components from D (Fig. 6(a) and Fig. 7(b)). Then the resulting polynomial $P_4(v, z)$ is given as

$$P_4(v, z) = vz \frac{v^{2n} - 1}{v^2 - 1} \cdot (v^{2n})^3 \cdot v^{2n-2}$$

Hence we obtain

$$P_4(v, z)H(D_4) = vz \frac{v^{2n} - 1}{v^2 - 1} v^{8n-2} \cdot \delta = v^{8n-2} - v^{10n-2}.$$

At last, we smooth $n - 1$ crossings of the other b_{2n-1}^γ and keep switching n crossings of each b_{2n}^α and one b_{2n-1}^γ , and then switch $n - 1$ crossings of the remaining b_{2n-1}^γ to obtain a trivial link diagram D_5 of two components from D (Fig. 6(a) and Fig. 7(b)). Then the resulting polynomial $P_5(v, z)H(D_5)$ is given as

$$P_5(v, z)H(D_5) = vz \frac{v^{2n-2} - 1}{v^2 - 1} \cdot (v^{2n})^3 \cdot v^{2n-2}$$

Hence we obtain

$$P_5(v, z)H(D_5) = vz \frac{v^{2n-2} - 1}{v^2 - 1} v^{8n-2} \delta = v^{8n-2} - v^{10n-4}.$$

According to the lemma 3.6, the lowest-degree term of z for $H(D(a_{2n}^\alpha, 2b_{2n}^\alpha, 3b_{2n-1}^\gamma))$ only contains the above five cases, hence we have

$$\begin{aligned} H_z^m(D) &= \prod_{i=1}^5 P_i(v, z)H(D_i) \\ &= v^{8n-2} + (v^{4n-2} - v^{6n-2}) + (v^{4n-2} - v^{6n-2}) + (v^{8n-2} - v^{10n-2}) + (v^{8n-2} - v^{10n-4}) \\ &= -v^{10n-2} - v^{10n-4} - 2v^{6n-2} + 3v^{8n-2} + 2v^{4n-2}. \end{aligned}$$

Theorem 3.11. *The link diagrams $D(2a_{2n}^\alpha, b_{2n}^\alpha, 3b_{2n-1}^\gamma)$, $D(3a_{2n}^\alpha, 3b_{2n-1}^\gamma)$ and $D(a_{2n}^\alpha, 3b_{2n-1}^\gamma, a_{2n}^{-\alpha}, b_{2n-1}^\gamma)$ are all chiral.*

Proof: For the link diagram $D = D(a_{2n}^\alpha, 3b_{2n-1}^\gamma, a_{2n}^{-\alpha}, b_{2n-1}^\gamma)$, by using theorem 3.10, we have

$$H_z^m(D) = H_z^m(D)(v, z) = (2v^{6n-4} - v^{4n-4})(v^{-1} - v)z^{-1}.$$

According to the property (2) of HOMFLY polynomial, we have

$$H_z^m(D^*) = H_z^m(D)(-v^{-1}, z) = (2v^{-6n+4} - v^{-4n+4})(v^{-1} - v)z^{-1}.$$

Then

$$H_z^m(D) \neq H_z^m(D^*).$$

Hence

$$H(D) \neq H(D^*).$$

Then $D(a_{2n}^\alpha, 3b_{2n-1}^\gamma, a_{2n}^{-\alpha}, b_{2n-1}^\gamma)$ is chiral. Similarly, the other four links can be shown to be chiral. ■

4 Discussion

In table 1, the crossing number, component number, twist number and chirality for 27 link types of OT-link diagrams are listed by using the results in last section. Note that the OT-link diagram $D(a_{2n}^\alpha, 3b_{2n}^\alpha, 2a_{2n}^\alpha)$ is a achiral link and is also the mirror image of $D(2a_{2n}^\alpha, 3b_{2n}^\alpha, a_{2n}^\alpha)$ by using theorem 3.1 and 3.2. Hence we obtain 26 link types for OT-link diagrams, which are differentiated by the crossing number, the component number, the chirality and HOMFLY polynomials. In table 1, for any two OT-link diagrams with the same crossing number and component number, they can be differentiated by the lowest-degree terms of z of HOMFLY polynomials provided in theorem 3.10. For example, $D(2a_{2n}^\alpha, 4b_{2n}^\alpha)$ and $D(a_{2n}^\alpha, 3b_{2n}^\alpha, a_{2n}^\alpha, b_{2n}^\alpha)$ have the same crossing number and component number. However, they represent two different link types due to their different HOMFLY polynomials by using theorem 3.10. Similarly for $D(a_{2n}^\alpha, 3b_{2n}^\alpha, 2a_{2n}^\alpha)$ and $D(2a_{2n}^\alpha, 3b_{2n}^\alpha, a_{2n}^\alpha)$, $D(3b_{2n}^\alpha, 3b_{2n-1}^\gamma)$ and $D(2a_{2n}^\alpha, b_{2n}^\alpha, 3b_{2n-1}^\gamma)$, $D(a_{2n}^\alpha, 2b_{2n}^\alpha, 3b_{2n-1}^\gamma)$ and $D(3a_{2n}^\alpha, 3b_{2n-1}^\gamma)$, and $D(b_{2n}^\alpha, 3b_{2n-1}^\gamma, b_{2n}^{-\alpha}, b_{2n-1}^\gamma)$ and $D(a_{2n}^\alpha, 3b_{2n-1}^\gamma, a_{2n}^{-\alpha}, b_{2n-1}^\gamma)$, each pair represent two different link types respectively. Hence we obtain the following theorem.

Theorem 4.1. *There are 26 different link types for OT-link diagrams listed in table 1.*

Among the 26 link types of OT-link diagrams, there are 22 link types of chiral links, which can be divided into 11 mirror-image pairs by using theorem 3.1. Note that any two mirror-image links have the same crossing number, component number and chirality except that their twist number have opposite signs. The remaining 4 link types for OT-links are all achiral, as shown in table 1. Moreover, among these OT-link diagrams, there are two link types with four components, five link types with three components, thirteen link types with two components and six link types with one component.

For the two link types of OT-link diagrams with four components, they have been synthesized by using four rationally designed oligonucleotides such that each oligonucleotide as a link component run around each face [5]. Note that these two link types of OT-link diagrams are mirror images of each other and hence both of them are chiral. This result confirms this possibility in experiment that there exists a pair of mirror isomers without considering the twist number on each edge.

For the OT-link diagrams with two or three components, there are seven link types such that each edge is composed of an oriented twist tangle a_{2n}^α or b_{2n}^α with even crossing number. For the remaining each OT-link diagram, there is at least an edge consisting of an oriented twist tangle with odd crossing number, that is a_{2n-1}^β or b_{2n-1}^γ . In particular for the OT-link diagram $D(2a_{2n-1}^\beta, b_{2n-1}^\gamma, a_{2n-1}^\beta, 2b_{2n-1}^\gamma)$, each edge can be formed by a half twist (for $n = 1$), which offer a possible candidate for synthesizing a smallest-size DNA polyhedron and achiral DNA polyhedron.

For the OT-link diagrams with one component, there are four link diagrams whose their twist number is a constant (0 or 3). Hence this number is independent on the complete twist number n of the oriented twist tangle on each edge. Moreover, among these OT-link diagrams, there are four link types of chiral links and two link types of achiral links. We note that a DNA tetrahedron with one component was realized recently by folding a single long strand of DNA [7]. However, this tetrahedron has a twin double helix on one edge, which is not the most compact structure. Our results provide multiple routes to assembled a DNA tetrahedron with the most compact structure by using a long DNA chain.

These works provide a list of candidates for synthesizing tetrahedral links with required topological structures, and also pave a way to design and determine the topological structures for polyhedral links with double-strands edges from theoretical viewpoint. However, there are still open problems need to be solved. For example, replacing tetrahedron with a polyhedron with low symmetry, it is also very hard to give all possible topological structures of the corresponding polyhedral links. Furthermore, it is still a challenge work to realize a polyhedral catenane without chiral structure.

Acknowledgments: This work was supported by a grant from the National Natural Science Foundation of China (No. 11501454).

References

- [1] N. C. Seeman, DNA in a material world, *Nature* **421** (2003) 427–431.
- [2] F. Zhang, J. Nangreave, Y. Liu, H. Yan, Structural DNA nanotechnology: state of the art and future perspective, *J. Am. Chem. Soc.* **136** (2014) 11198–11211.
- [3] M. R. Jones, N. C. Seeman, C. A. Mirkin, Programmable materials and the nature of the DNA bond, *Science* **347** (2015) #1260901.
- [4] R. P. Goodman, R. M. Berry, A. J. Turberfield, The single–steps synthesis of a DNA tetrahedron, *Chem. Commun.* **12** (2004) 1372–1373.
- [5] R. P. Goodman, I. A. T. Schaap, C. F. Tardin, C. M. Erben, R. M. Berry, C. F. Schmidt, A. J. Turberfield, Rapid chiral assembly of rigid DNA building blocks for molecular nanofabrication, *Science* **310** (2005) 1661–1665.
- [6] Y. He, T. Ye, M. Su, C. Zhang, A. E. Ribbe, W. Jiang, C. D. Mao, Hierarchical self–assembly of DNA into symmetric supramolecular polyhedral, *Nature* **452** (2008) 198–201.
- [7] Z. Li, B. Wei, J. Nangreave, C. Lin, Y. Liu, Y. Mi, H. Yan, A replicable tetrahedral nanostructure self-assembled from a single DNA strand, *J. Am. Chem. Soc.* **131** (2009) 13093–13098.
- [8] T. Kato, R. P. Goodman, C. M. Erben, A. J. Turberfield, K. Namba, High–resolution structural analysis of a DNA nanostructure by cryoEM, *Nano Lett.* **9** (2009) 2747–2750.
- [9] Y. Ke, J. Sharma, M. Liu, K. Jahn, Y. Liu, H. Yan, Scaffolded DNA origami of a DNA tetrahedron molecular container, *Nano Lett.* **9** (2009) 2445–2447.
- [10] J. Chen, N. C. Seeman, The electrophoretic properties of a DNA cube and its substructure catenanes, *Nature* **350** (1991) 631–633.
- [11] C. Zhang, S. H. Ko, M. Su, Y. J. Leng, A. E. Ribbe, W. Jiang, C. D. Mao, Symmetry controls the face geometry of DNA polyhedra, *J. Am. Chem. Soc.* **131** (2009) 1413–1415.
- [12] W. M. Shih, J. D. Quispe, G. F. Joyce, A 1.7-kilobase single–stranded DNA that folds into a nanoscale octahedron, *Nature* **427** (2004) 618–621.
- [13] F. F. Andersen, B. Knudsen, C. L. P. Oliveira, R. F. Fröhlich, D. Krüger, J. Bungert, M. Agbandje-McKenna, R. McKenna, S. Juul, C. Veigaard, J. Koch, J. L. Rubinstein, B. Guldbbrandtsen, M. S. Hede, G. Karlsson, A. H. Andersen, J. S. Pedersen, B. R.

- Knudsen, Assembly and structural analysis of a covalently closed nano-scale DNA cage, *Nucleic Acids Res.* **36** (2008) 1113–1119.
- [14] Y. He, M. Su, P. A. Fang, C. Zhang, A. E. Ribbe, W. Jiang, C. D. Mao, On the chirality of self assembled DNA octahedra, *Angew. Chem. Int. Ed.* **49** (2010) 748–751.
- [15] J. Zimmermann, M. P. J. Cebulla, S. Möninghoff, G. V. Kiedrowski, Self-assembly of a DNA dodecahedron from 20 trisologonucleotides with C3h linkers, *Angew. Chem. Int. Ed.* **47** (2008) 3626–3630.
- [16] C. Zhang, M. Su, Y. He, X. Zhao, P. A. Fang, A. E. Ribbe, W. Jiang, C. D. Mao, Conformational flexibility facilitates self-assembly of complex DNA nanostructures, *Proc. Natl. Acad. Sci. USA* **105** (2008) 10665–10669.
- [17] D. Bhatia, S. Mehtab, R. Krishnan, S. S. Indi, A. Basu, Y. Krishnan, Icosahedral nanocapsules by modular assembly, Icosahedral DNA nanocapsules via modular assembly, *Angew. Chem. Int. Ed.* **48** (2009) 4134–4137.
- [18] C. L. P. Oliveira, S. Juul, H. L. Jørgensen, B. Knudsen, D. Tordrup, F. Oteri, M. Falconi, J. Koch, A. Desideri, J. S. Pedersen, F. F. Andersen, B. R. Knudsen, Structure of nanoscale truncated octahedral DNA cages: Variation of single stranded linker regions and influence on assembly yields, *ACS Nano.* **4** (2010) 1367–13376.
- [19] A. R. Chandrasekaran, O. Levchenko, DNA nanocages, *Chem. Mater.* **28** (2016) 5569–5581.
- [20] N. Xie, S. Liu, X. Yang, X. He, J. Huang, K. Wang, DNA tetrahedron nanostructures for biological applications: biosensors and drug delivery, *Analyst* **142** (2017) 3322–3332.
- [21] Y. Hu, Z. Chen, H. Zhang, M. Li, Z. Hou, X. Luo, X. Xue, Development of DNA tetrahedron-based drug delivery system, *Drug Delivery* **24** (2017) 1295–1301.
- [22] P. R. Cromwell, *Knots and Links*, Cambridge Univ. Press, Cambridge, 2004.
- [23] P. D. Tumasnia, J. I. Sulkowska, Topological knots and links in proteins, *Proc. Nad. Acad. Sci. USA* **114** (2017) 3415–3420.
- [24] J. H. White, N. R. Cozzarelli, A simple topological method for describing stereoisomers of DNA catenanes and knots, *Proc. Nad. Acad. Sci. USA* **81** (1984) 3322–3326.
- [25] W. Qiu, Z. Wang, G. Hu, *The Chemistry and Mathematics of DNA Polyhedra*, Nova, New York, 2010.

- [26] W. Qiu, X. Zhai, Molecular design of Goldberg polyhedral links, *J. Mol. Struct. (Theochem)* **756** (2005) 163–166.
- [27] G. Hu, X. D. Zhai, D. Lu, W. Y. Qiu, The architecture of Platonic polyhedral links, *J. Math. Chem.* **46** (2009) 592–603.
- [28] G. Hu, W. Qiu, A. Ceulemans, A new Euler’s formula for DNA polyhedra, *PLOS One* **6** (2011) #e26308.
- [29] J. Duan, W. Qiu, Using dual polyhedral links models to predict characters of DNA polyhedra, *J. Mol. Struct.* **359** (2013) 233–236.
- [30] X. S. Cheng, W. Y. Qiu, H. P. Zhang, A novel molecular design of polyhedral links and their chiral analysis, *MATCH Commun. Math. Comput. Chem.* **62** (2013) 725–742.
- [31] S. Liu, H. Zhang, Genera of the links derived from 2-connected plane graphs, *J. Knot Theory Ramif.* **21** (2014) #1250129.
- [32] X. Cheng, H. Zhang, X. Jin, W. Qiu, Ear decomposition of 3-regular polyhedral links with applications, *J. Theor. Biol.* **359** (2014) 146–154.
- [33] S. Jablan, L. Radović, R. Sazdanović, Knots and links derived from prismatic graphs, *MATCH Commun. Math. Comput. Chem.* **66** (2010) 65–92.
- [34] G. Hu, W. Qiu, X. Cheng, S. Liu, The complexity of Platonic and Archimedean polyhedral links, *J. Math. Chem.* **48** (2010) 401–412.
- [35] S. Liu, X. Cheng, H. Zhang, W. Qiu, The architecture of polyhedral links and their Homfly polynomials, *J. Math. Chem.* **48** (2010) 439–456.
- [36] X. Jin, F. Zhang, The Homfly polynomial for even polyhedral links, *MATCH Commun. Math. Comput. Chem.* **63** (2010) 657–677.
- [37] S. Liu, H. Zhang, W. Qiu, The Homfly polynomial for a family of polyhedral links, *MATCH Commun. Math. Comput. Chem.* **67** (2012) 65–90.
- [38] X. Cheng, X. Jiang, H. Dai, The braid index of polyhedral links, *J. Math. Chem.* **50** (2012) 1386–1397.
- [39] S. Liu, H. Zhang, Some invariants of polyhedral links, *MATCH Commun. Math. Comput. Chem.* **70** (2013) 383–400.
- [40] X. Cheng, X. Jin, The braid index of complicated DNA polyhedral links, *PLOS One* **7** (2012) #e48968.

- [41] M. Li, Q. Deng, X. Jin, A general method for computing the Homfly polynomial of DNA double crossover 3-regular links, *PLOS One* **10** (2015) #e0125184.
- [42] G. Hu, Z. Wang, W. Qiu, A survey on mathematical models for DNA polyhedra, *MATCH Commun. Math. Comput. Chem.* **70** (2013) 725–742.
- [43] X. Jin, A survey on several invariants of three types of polyhedral links, *MATCH Commun. Math. Comput. Chem.* **76** (2016) 569–594.
- [44] S. Liu, H. Zhang, The HOMFLY polynomials of odd polyhedral links, *J. Math. Chem.* **51** (2013) 1310–1328.
- [45] M. Bon, G. Vernizzi, H. Orland, A. Zee, Topological classification of RNA structures, *J. Mol. Biol.* **379** (2008) 900–911.
- [46] C. Cerf, A. Stasiak, A topological invariant to predict the three-dimensional writhe of ideal configurations of knots and links, *Proc. Nad. Acad. Sci. USA* **97** (2000) 3795–3798.
- [47] L. H. Kauffman, State models and the Jones polynomial, *Topology* **26** (1987) 395–407.
- [48] P. Freyd, D. Yetter, J. Hoste, W. B. R. Lickorish, K. Millett, A. Ocneanu, A new polynomial invariant of knots and links, *Bull. Amer. Math. Soc.* **12** (1985) 239–246.
- [49] J. H. Przytycki, P. Traczyk, Invariants of links of Conway type, *Kobe J. Math.* **4** (1987) 115–139.
- [50] F. Jaeger, A combinatorial model for the Homfly polynomial, *Eur. J. Comb.* **11** (1990) 549–558.
- [51] D. B. West, *Introduction to Graph Theory*, Prentice Hall, New Jersey, 2001.
- [52] E. Steinitz, Polyeder und Raumeinteilungen, *Enzykl. Math. Wiss. (Geometrie)* **3** (1922) 1–139.